energies

MDPI

Review

Applications of Supercritical Water in Waste Treatment and Valorization: A Review

Nadjiba Benmakhlouf [1], Nawel Outili [1], Belén García-Jarana [2], Jezabel Sánchez-Oneto [2], Juan R. Portela [2], Mejdi Jeguirim [3,*] and Abdeslam-Hassen Meniai [1]

[1] Environmental Process Engineering Laboratory, University Constantine 3, Constantine 25000, Algeria
[2] Department of Chemical Engineering and Food Technology, University of Cadiz, 11003 Cádiz, Spain
[3] Institut de Sciences des Matériaux de Mulhouse, Université de Haute-Alsace, 68100 Mulhouse, France
* Correspondence: mejdi.jeguirim@uha.fr; Tel.: +33-(0)-3-89-33-67-61

Abstract: The present review deals with water applications in sub and supercritical conditions with a focus on supercritical water oxidation process (SCWO) as an example of high temperature and pressure technologies. It starts by presenting the advantages of water properties near and beyond the critical point and the major applications exploiting them. Then, it presents a review on SCWO from the description of the process, the reaction mechanism and kinetics to reactor design and modeling. It also presents the main problems and difficulties that delay the SCWO industrial application, and summarizes the main efforts and research to overcome them for a safe, efficient and economic process.

Keywords: supercritical water applications; hydrothermal oxidation; supercritical water properties; chemical kinetics; modeling; SCWO

Citation: Benmakhlouf, N.; Outili, N.; García-Jarana, B.; Sánchez-Oneto, J.; Portela, J.R.; Jeguirim, M.; Meniai, A.-H. Applications of Supercritical Water in Waste Treatment and Valorization: A Review. *Energies* **2023**, *16*, 2081. https://doi.org/10.3390/en16042081

Academic Editor: Gabriele Di Giacomo

Received: 3 January 2023
Revised: 10 February 2023
Accepted: 14 February 2023
Published: 20 February 2023

1. Introduction

Large quantities of waste from different sources pose considerable environmental problems and must be eliminated by efficient techniques and with control of effluents that respect the environment. The use of supercritical fluids for this purpose meets these criteria and the most commonly used are water and carbon dioxide and less frequently, methanol, ethane, ethene, butene and pentane [1]. Figure 1 shows a comparison of number of international Patent Cooperation Treaty (PCT) with supercritical water and CO_2 for the period from 1981 to 2019.

The basic concept of this technology is the exploitation of these fluids at high temperature and pressure as a reaction medium [2]. The increase in temperature and pressure of water near subcritical conditions (temperature between 150 °C and 230 °C and pressure between 20 and 150) or beyond the critical point of water (temperature 374 °C and pressure 22.1 MPa) radically changes its physicochemical properties.

They take an intermediate value between those of the liquid and gas at standard conditions [1]. Moreover, its properties became tunable and permit the reduction of diffusion limitations of the reaction kinetics, making water under these conditions an attractive reaction media. It also provides solutions to several problems related to biological reactions such as cell lysis, sterilization and virus inactivation [3]. With the appearance of green chemistry principles, supercritical fluids became more attractive as a suitable alternative for conventional solvents and were considered to be "green solvents". Supercritical fluids meet the specifications of green solvents since they have low toxicity, can be reused, ensure great efficiency and can mediate reactions, separations and catalyst recycling [4].

These new properties lead to new applications of sub and supercritical water in several fields: waste treatment and environmental applications, biomass valuation, renewable energy, materials, pharmaceutical, biomedical and agrifood applications [3,5].

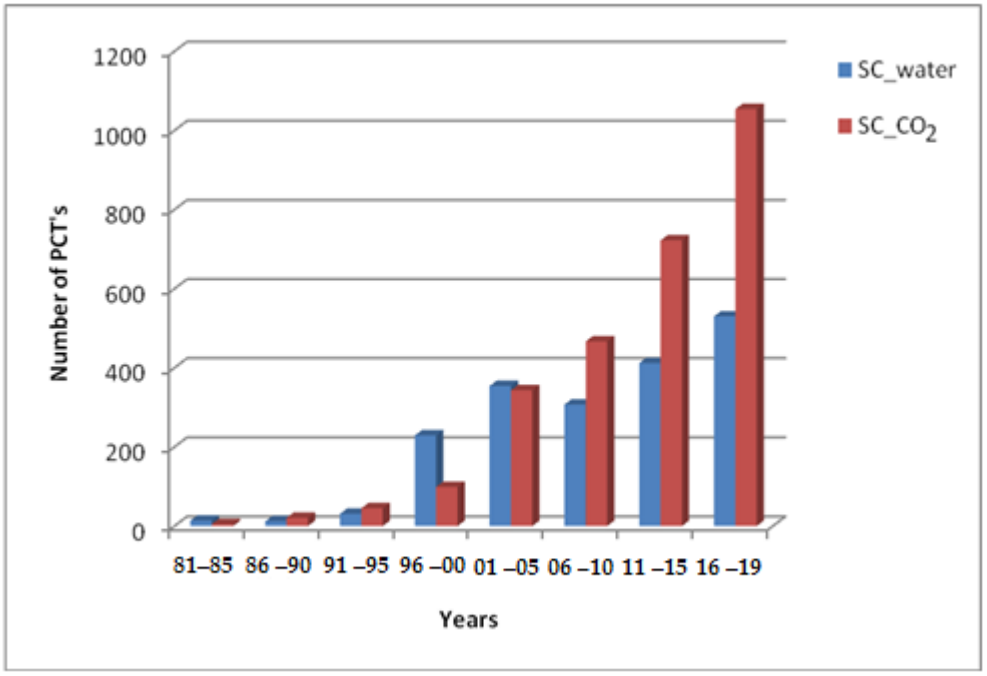

Figure 1. Number of PCT with Sc-water and SC-CO_2 for the period from 1981 to 2019 (from PATENTSCOPE-World Intellectual Property Organization (WIPO) database of international PCT applications).

The idea of supercritical water for waste treatment appeared in the late 1970s and research accelerated in the 1980s [6], where it had become an attractive support for several applications, particularly in the field of wastewater treatment. Michael Modell extended the work of destroying toxic and dangerous waste and created the MODAR Company to market the process [7,8].

Often known for the treatment of waste in supercritical water oxidation (SCWO) [9] and also subcritical water oxidation, named wet air oxidation (WAO) [10], subcritical or supercritical water is increasingly studied for its ability to promote hydrolysis reactions by breaking the carbon chain [11]. In the energy field, the use of subcritical or supercritical water for the production of biofuels, biogas, or even hydrogen-rich gas offers relevant solutions to fossil energy replacement [12]. The extraction of bioactive compounds or natural essences by subcritical water is also an area of application which has attracted a lot of attention and has made it possible to extract many compounds of great medical, pharmaceutical, cosmetic and food interest [1,5,11,13,14].

Supercritical water oxidation (SCWO) is a waste treatment method that can convert hazardous organics completely and quickly into water and carbon dioxide [2]. The supercritical water oxidation (SCWO) process is based on the oxidation of waste in supercritical water conditions. At these conditions, water became a perfect medium for reaction due to its low density, low viscosity, low dielectric constant and high diffusivity and miscibility with organics and oxygen [2,15]. Under these new conditions, water acquires new advantages by ensuring a single-phase reaction medium without limitations to transfer, an increase in reaction and pollutant oxidation rates (elimination efficiencies that can reach 99.99%) [3], and the final liquid effluent is non-toxic and can be discharged without treatment [4–18]. The gas effluent is also clear, carbon monoxide content is just a few parts per million [19] and as the result of the almost low temperatures of the SCWO process (400–650 °C), none of the NOx compounds are generated compared to the incineration process (900–1300 °C) [9,20,21].

The SCWO reaction is highly exothermic, which makes the process interesting from an energetic point of view with the possibility of recovering the heat released by the reaction with a view to making the process auto-energetic [10].

Several research studies have been carried out to test the effectiveness of this technology for the destruction of many organic compounds, an early patent for the process included destruction of many pollutants such as dodecane [11,12], PCB (polychlorinated biphenyls) [13], phenol [14,15], Acetic Acid [16], cutting oil [17–20], methanol [11,21,22] and landfill leachate [23]. These tests have been implemented on a laboratory and/or pilot scale in different types of reactors.

However, the SCWO presents difficulties which delay the extension of its application to the industrial scale, such as corrosion, salt precipitation due to the operating conditions in pressure and supercritical temperature, and the investment cost [24]. For these reasons, much research has been conducted to make improvements to overcome these difficulties.

2. Properties of Supercritical Water

In supercritical water, the properties differ significantly from those of ordinary liquid water or steam. The density changes rapidly, and its evolution presents a large gradient at the critical point; it takes an intermediate value between that of water in the liquid state (1 g/cm^3) and that in the gaseous state (0.001 g/cm^3) [1], the density of water affects the solubility of organic compounds and gases, this point is therefore particularly important [25]. The viscosity of supercritical water is reduced and the diffusivities are usually high [26].

Modifications in structure and bonding as a function of temperature and pressure are followed by variations of the dielectric constant of water that can function as an acid or basic catalyst [27]. The static dielectric constant drops from 78.5 F/m at 25 °C to 5 F/m near the critical region to 1–2 F/m at 450 °C [28] due to the reduction of hydrogen bonds number [29]. This leads the supercritical water (SCW) to act as a non-polar medium, and its solvation characteristics become similar those of a reduced polarity organic solvent [18]. Thereby, SCW is absolutely miscible with gases like N_2, O_2, and CO_2 [30]. In contrast, inorganic salts are nearly insoluble in SCW [31].

Concerning thermal properties, they vary sharply at the critical point. Thermal conductivity decreases, which, from the process viewpoint, indicates that heat exchanges will be less efficient than those for water in ambient conditions [2], and the calorific capacity of water becomes infinite at the critical point. Accordingly, near the critical temperature, it is necessary to provide more energy to the fluid to increase temperature [22].

Combining the solvation and new physical properties transforms supercritical water into a perfect medium for the oxidation reaction of organic pollutants. The dissolution of organic compounds and oxygen in supercritical water ensure rapidly an infinite molecular contact in a single phase without mass transfer limitations, resulting in faster kinetics and completion of oxidation [32].

Estimating the thermodynamic properties of aqueous systems in the vicinity of the critical water point is, therefore, a challenging task. Interest in modeling of the SCWO processes has grown in recent years. Models have been developed that take into account mass, momentum and energy balances to promote the understanding of sub-and supercritical systems, their scaling and reaction heat integration [26,33–35]. Precise values of density, viscosity, enthalpy, and heat capacity are required for both water and aqueous mixtures in order to obtain accurate results of this type of model. Also, an accurate evaluation of the thermo-physical properties is needed, and, therefore, the interest in a state equation (EOS) capable of describing SCWO systems is growing [36]. Current cubic EOS are not very accurate in sub and supercritical states, although Peng and Robinson's EOS, with the translated volume correction, are capable of estimating the density of the water-air system and describing the behavior of the SCWO reactors quite accurately [19]. For the estimation of thermal conductivity and viscosity, Sengers et al. [37] proposed the equations of the thermal conductivity and viscosity as a function of the temperature and the density. For this purpose, the correlations proposed by Chung [38] can also be used [19].

The most used formulation for calculating the properties of supercritical water was that of the International Association for Properties of Water and Steam (IAPWS)-IF 97 which allows the estimation of water density, viscosity, thermal conductivity, enthalpy,

calorific capacity and dielectric constant for different temperature (T) and pressure (P). This formulation is a set of equations for various regions that cover the following interval of validity of T and P [39]:

$$273.15 \leq T \leq 1073.15 \text{ K et } P \leq 100 \text{ MPa and } 1073.15 \leq T \leq 2273.15 \text{ K et } P \leq 10 \text{ MPa}$$

Figure 2 shows the five regions that make up the whole range of validity of IAPWS-IF97, in this formulation each zone is represented by a fundamental equation, as shown in Table 1.

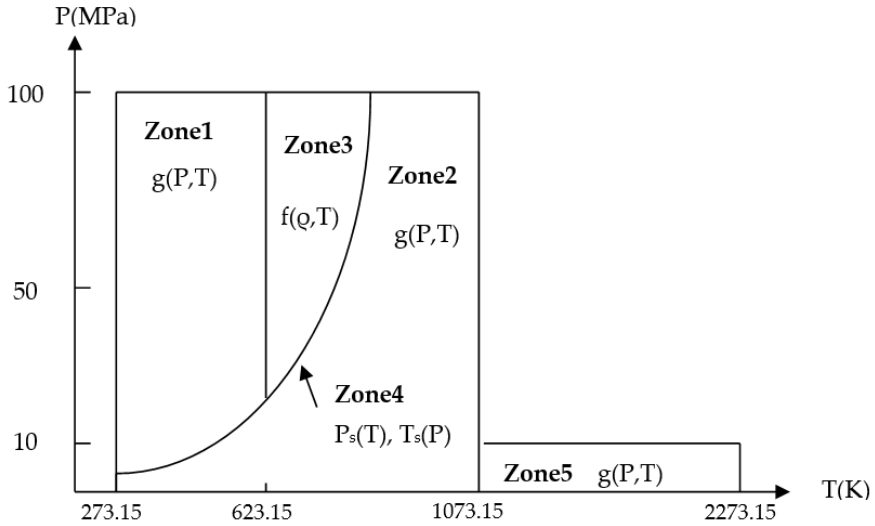

Figure 2. The five regions and equations of IAPWS-IF97 [39].

Table 1. Equations for calculation of supercritical water properties.

Zone	Temperature Range (K)	Pressure Range (Mpa)	Gibbs and Helmholtz Free Energies and Saturation Pressure for Supercritical Water Properties Calculation
1	[273.15, 623.15]	[P_{sat} (T) 100]	Gibbs free energy as:
			$g1(T,P) = R{\cdot}T{\cdot}\sum_{i=1}^{34} n_i{\cdot}\left(7.1 - \frac{P}{P^*}\right)^{I_i}{\cdot}\left(\frac{T^*}{T} - 1.222\right)^{J_i}$ (1)
			T (K), P (MPa), R the universal gas constant ($kJ{\cdot}kg^{-1}{\cdot}K^{-1}$), n_i, I_i and J_i tabulated constants, P* = 16.53 MPa, T* =1383 K and R = 0.461526 $kJ{\cdot}kg^{-1}{\cdot}K^{-1}$
2	[273.15, 623.15] [623.15, 863.15] [863.15, 073.15]	[0, P_{sat} (T)] [0, $P_{2/3}$ (T)] [0, 100]	$\frac{P_{2/3}}{P^*} = n_1 + n_2{\cdot}\frac{T}{T^*} + n_3{\cdot}\left(\frac{T}{T^*}\right)^2$ (2)
			With P* = 1 Pa, T* = 1 K, n_1, n_2 and n_3 are obtained from Tables.
			The water properties are also calculated from g, the Gibbs free energy expressed as:
			$\frac{g2(T,P)}{R.T} = \gamma\left(\frac{P}{P^*}, \frac{T^*}{T}\right) = \gamma^0 + \gamma^r$ (3)
			With γ^0 and γ^r the dimensionless (ideal) and residual activity coefficients, respectively, and are expressed as follows:
			$\gamma^0 = \ln{\cdot}\left(\frac{P}{P^*}\right) + \sum_{i=1}^{9} n_i^0{\cdot}\left(\frac{T^*}{T}\right)^{J_i^0}$ (4)
			$\gamma^r = \sum_{i=1}^{43} n_i{\cdot}\left(\frac{P}{P^*}\right)^{I_i}{\cdot}\left(\frac{T^*}{T} - 0.5\right)^{J_i}$ (5)
			with P* = 1 MPa, T* = 540 K, n_i^0, n_i, J_i and J_i^0 are reported in [39].

Table 1. *Cont.*

Zone	Temperature Range (K)	Pressure Range (Mpa)	Gibbs and Helmholtz Free Energies and Saturation Pressure for Supercritical Water Properties Calculation
3	[623.15, 863.15]	[$P_{2/3}$ (T), 100]	$P_{2/3}$(T) is calculated from Equation (2). Water properties are calculated using Helmholtz free energy f, expressed as: $f3(T,\rho) = R{\cdot}T{\cdot}\left(n_1{\cdot}\ln\left(\frac{\rho}{\rho^*}\right) + \sum_{i=2}^{40} n_i{\cdot}\left(\frac{\rho}{\rho^*}\right)^{I_i}{\cdot}\left(\frac{T^*}{T}\right)^{J_i}\right)$ (6) With $\rho^* = \rho_c = 322\ kg/m^3$, $T^* = T_c = 647.096$ K, $R = 0.461526\ kJ{\cdot}kg^{-1}{\cdot}K^{-1}$, n_i, J_i and I_i from tables in appendice). ρ_c: density of pure water at the critical T_c
4	[273.15, 647.096]		This zone corresponds to the vapor-liquid phase equilibria and the saturation pressure is calculated as: $P_{sat} = P^*{\cdot}\left[\frac{2.C}{-B+\left(B^2-4{\cdot}A{\cdot}C\right)^{0.5}}\right]^4$ (7) - $A = \upsilon^2 + n_1{\cdot}\upsilon + n_2$ - $B = n_3{\cdot}\upsilon^2 + n_4.\upsilon + 5$ - $C = n_6{\cdot}\upsilon^2 + n_7{\cdot}\upsilon + n_2$ - $\upsilon = (T/T^*) + (n_9/((T/T^*) - n_{10}))$ $P^* = 1$ MPa, $T^* = 1$ K, coefficients n_i are reported in [39].
5	[1073.15, 273.15]	[0, 100]	The water properties are calculated from g, similarly to the case of Zone 2, using Equations (1)–(6) but with a different coefficients (n_i^0, J_i^0, n_i, J_i).

The two regions, one and two, are independently covered by a basic Gibbs free energy equation g (T, P), the third region is covered by a fundamental Helmholtz free energy equation f (ρ, T) where ρ is the density. The saturation state is covered by a saturation-pressure equation Ps (T). Finally, zone five is covered by the equation g (T, P) [39,40].

This IAPW-IF-97 formulation was successfully used by many researchers in their work on the SCWO reactor modeling studies: A. Fourcault et al. [33], J. Mercadier et al. [34], Jan A.M. Withag et al. [41], J.P. Serin et al. [42], where they supposed that the mixture properties are equal to a pure water, than they calculates them from this formulation in their models. The following Table 2 shows the equations used in the supercritical water properties:

Table 2. Equations of supercritical water property calculations.

Property	Supercritical Water Property Calculation
Density	- Using Gibbs free energy g:
	$\frac{1}{\rho} = \left(\frac{\partial g}{\partial P}\right)_T$ (8)
	- Using Helmholtz f:
	$\rho = P - \rho^2{\cdot}\left(\frac{\partial f}{\partial \rho}\right)_T$ (9)
Heat capacity	$C_p = \left(\frac{\partial h}{\partial T}\right)_P$ (10) h the enthalpy. Using Gibbs free energy: $h = g - T{\cdot}\left(\frac{\partial g}{\partial T}\right)_P$ (11) Using Helmholtz free energy: $h = f - T{\cdot}\left(\frac{\partial f}{\partial T}\right)_\rho + \rho{\cdot}\left(\frac{\partial f}{\partial \rho}\right)_T$ (12)

Table 2. *Cont.*

Property	Supercritical Water Property Calculation	
Dielectric constant	$\varepsilon(T,\rho) = \frac{1+A+5B+\left(9+2A+18B+A^2+10AB+9B^2\right)^{0.5}}{4\cdot(1-B)}$	(13)
	$A = \frac{N_A\cdot\mu^2\cdot\rho\cdot G}{M\cdot\varepsilon_0\cdot k\cdot T}$	(14)
	$B = \frac{N_A\cdot\rho\cdot\alpha}{3\cdot M\cdot\varepsilon_0}$	(15)
	$G = 1+\sum_{i=1}^{11} n_i\cdot\delta^{I_i}\cdot\tau^{J_i} + n_{12}\cdot\delta\cdot\left(\frac{T_c}{288k}\cdot\tau^{-1}\right)^{-1.2}$	(16)
	$\Delta = \rho/\rho^*$, $\tau = T^*/T$, $\rho^* = \rho_c = 322\ kg/m^3$, $T^* = T_c = 647.096\ K$, $\lambda^* = 1\ Wm^{-1}K^{-1}$	
Viscosity	$\frac{\mu(T,\rho)}{\mu^*} = \psi_0(\theta)\cdot\psi_1(\delta,\theta)$	(17)
	$\psi_0(\theta) = (\theta)^{0.5}\cdot\left[\sum_{i=1}^{4} n_i^0\cdot(\theta)^{1-i}\right]^{-1}$	(18)
	$\psi_1(\delta,\theta) = \exp\cdot\left[\delta\cdot\sum_{i=1}^{21} n_i\cdot\left(\frac{\rho}{\rho^*}-1\right)^{I_i}\cdot\left((\theta)^{-1}-1\right)^{J_i}\right]$	(19)
	- $\delta = \rho/\rho^*$, $\theta = T/T^*$, $\rho^* = \rho_c = 322\ kg/m^3$, $T^* = T_c = 647.096\ K$, $\mu^* = 1\times10^{-4}\ Pa\cdot s$	
	- Coefficients n_i^0, n_i, I_i, and J_i, are reported in [39].	
Thermal conductivity	$\frac{\lambda}{\lambda^*} = \Lambda_0(\theta)+\Lambda_1(\delta)+\Lambda_2(\delta,\theta)$	(20)
	$\Lambda_0(\theta) = \theta^{0.5}\cdot\sum_{i=1}^{4} n_i^0\cdot\theta^{i-1}$	(21)
	$\Lambda_1(\delta) = n_1+n_2\cdot\delta+n_3\cdot\exp\left[n_4\cdot(\delta+n_5)^2\right]$	(22)
	$\Lambda_2(\delta,\theta) = \left(n_1\cdot\theta^{-10}+n_2\right)\cdot\delta^{1.8}\cdot\exp\left[n_3\cdot\left(1-\delta^{2.8}\right)\right]+n_4\cdot A\cdot\delta^B\cdot\exp\left[\left(\frac{B}{B+1}\right)\cdot\left(1-\delta^{1+B}\right)\right]+ n_5\cdot\exp\left[n_6\cdot\theta^{1.5}+n_7\cdot\delta^{-5}\right]$	(23)
	$A = 2+n_8\cdot(\Delta\theta)^{-0.6}$	(24a)
	$B = \begin{cases}(\Delta\theta)^{-1} & \text{si } \theta\geq 1\\ n_9\cdot(\Delta\theta)^{-0.6} & \text{si } \theta<1\end{cases}$	(24b)
	$\Delta\theta = \lvert\theta-1\rvert+n_{10}$	(24c)
	$\delta = \rho/\rho^*$, $\theta = T^*/T$, $\rho^* = 317.7\ kg/m^3$, $T^* = T_c = 647.096\ K$, $\lambda^* = 1\ Wm^{-1}K^{-1}$	
	Coefficients n_i^0, n_i, I_i, and J_i, are reported in [39].	

Experimental data are available and tabulated following NIST standards. This approach is precise since it is based on experimental values. In the present work, a model along with a computing code using Mathcad have been developed from the formulation of the IAPWS for calculating all proprieties. This is justified by the fact that data files from NIST cannot be called from the code.

The following Figure 3 presents the values of the variation of water properties around the critical point as a function of T and P as obtained from the developed Mathcad code [40].

The plots of Figure 3 show the variations of the considered supercritical water properties with temperature are physically consistent. For instance, an increase in temperature leads to an enthalpy increase and density, dynamic viscosity, dielectric constant, etc., confirming the reliability of the used equations.

The properties obtained using NIST and the developed Mathcad code are shown in Table 3 as follows:

Table 3. Comparison of water properties using IAPWS and the developed program.

Region	T (K)	P (MPa)	From the Developed Code	Test Value [1]	Test Value (NIST [2])
			ρ (kg/m^3)		
1	300	0.3	997.85294010	997.85293979	997.85
2	700	30	184.18016876	184.18016892	184.24
3	750	78.3095639	499.99999993	500	499.95
5	1500	30	43.33482271	43.33482279	43.337

Table 3. *Cont.*

Region	T (K)	P (MPa)	From the Developed Code	Test Value [1]	Test Value (NIST [2])
			μ (Pa·s)		
1	298.15	0.1	$8.90022551 \times 10^{-4}$	$8.90022551 \times 10^{-4}$	8.9002×10^{-4}
2	873.15	20	$3.39743835 \times 10^{-5}$	$3.39743835 \times 10^{-5}$	3.3974×10^{-5}
3	673.15	60	$7.26093560 \times 10^{-5}$	$7.26093560 \times 10^{-5}$	7.2613×10^{-5}
			Cp (J/g·K)		
1	300	0.3	4.17301218	4.17301218	4.1725
2	700	30	10.35050922	10.3505092	10.351
3	650	25.5837018	13.89357179	13.8935717	13.893
5	1500	0.5	2.61609445	2.61609445	2.6157
			h (kJ/kg)		
1	300	0.3	115.33127302	115.331273	115.32
2	300	0.0035	2549.91145084	2549.91145	2549.9
3	650	25.5837018	1863.43019020	1863.43019	1863.5
5	1500	30	5167.23514008	5167.23514	5167.3
			ε (F/m)		
1	298.15	5	78.04662743	78.5907250	/
2	873.15	10	1.12620467	1.12620970	/
3	673.15	40	10.30623674	10.3126058	/
			k (W/m K)		
1	298.15	0.1	0.60750981	0.607509806	0.60652
2	873.15	10	0.08671962	0.08675703	0.087077
3	673.15	40	0.39422663	0.398506911	0.41256

ρ: Density (kg/m^3), μ: Dynamic viscosity (Pa s), Cp: Heat capacity (J/g K), h: Enthalpy (kJ/kg), ε: Constant dielectric, (F/m), k: Thermal conductivity (W/(m K)).

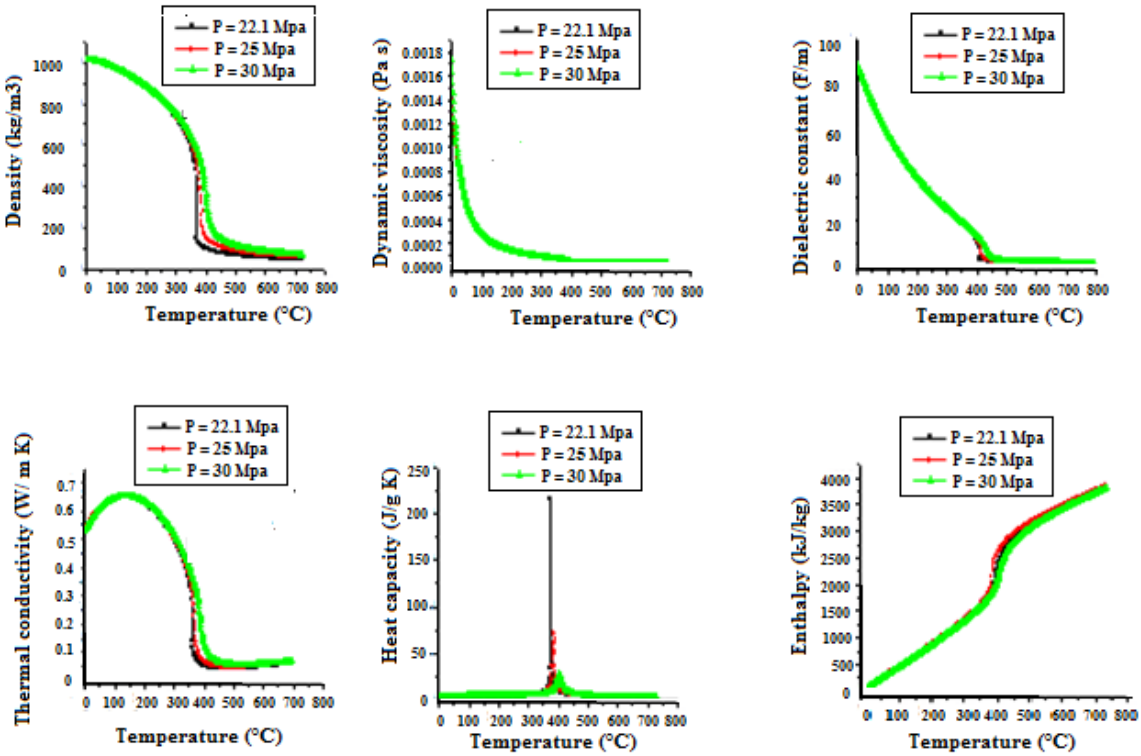

Figure 3. Properties of water around supercritical conditions.

This IAPW-IF 97 formulation was successfully used by many researchers in their works on the SCWO reactor modeling studies by A. Fourcault et al. [33], J. Mercadier et al. [34], Jan A.M. Withag et al. [41], J.P. Serin et al. [42], where they supposed that the mixture properties are equal to those of a pure water, then they calculated them from this formulation in their models.

3. Supercritical and Subcritical Water Applications

In addition to supercritical and subcritical water oxidation for waste treatment, new properties of water at these conditions were exploited in several applications. Figure 4 summarizes the main processes using water beyond or near its critical point.

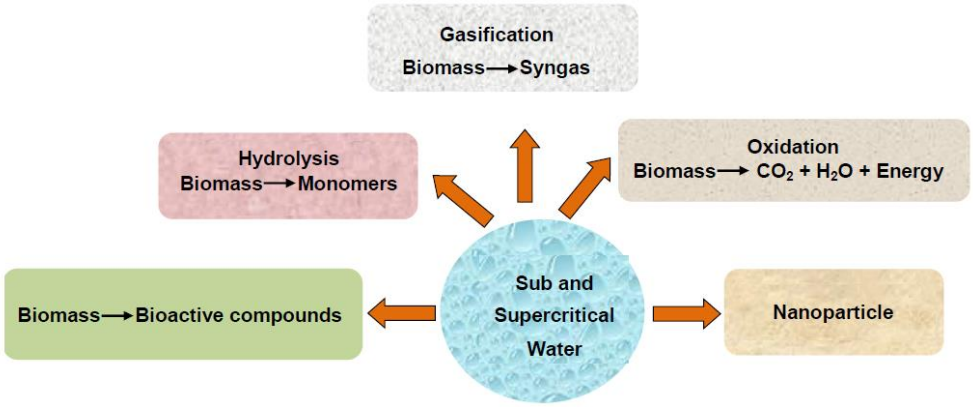

Figure 4. Main sub and supercritical water applications.

In sub or supercritical water, extraction performance increases due to the increase of mid-polar compounds solubility in terms of temperature and pressure, which allows the reduction of organic solvent use [11]. Therefore, it is easier to dissolve certain bioactive compounds in water in the subcritical state than in water under standard conditions. Furthermore, the tunability of water properties allows the extraction of specific bioactive compounds, selection of specific operating conditions and respects biodegradation conditions. This technology, especially subcritical water extraction, had been used by several researchers to extract polyphenols, antioxidants, flavonoids, acids and other bioactive compounds from plants and vegetable raw materials [11,13]. Supercritical and subcritical water extraction was used to recover natural compounds from various raw materials, such as the different parts of a given plant, food byproducts, algae and microalgae [43].

In recent years, sub and supercritical water hydrolysis had replaced conventional technologies to convert biomass into sugars for biofuels production [12]. Hemicellulose and cellulose were the most used biomass, but they respond differently to hydrothermal treatment. On the other hand, Lignin was the most recalcitrant biomass. The maximum sugar yield was obtained for hemicelluloses at 220–235 °C [44] while the hydrolysis of Cellulose was mainly observed at temperatures from 320 to 350 °C [11].

Hydrothermal carbonization is the hydrolysis of saccharides in subcritical water used to replace pyrolysis of wet biomass at lower temperatures to produce char with maximum yield at temperatures in the range of 150 to 300 °C [45]. Hydrogen storage capacities of hydrothermal carbonized organic compounds were very promising for this application [46].

Supercritical water was also used in the depolymerization or decomposition of plastics as an effective solution for recycling and recovering one of the most polluting wastes of the environment. When biomass is treated in supercritical water, hydrolysis takes place more efficiently [29].

The SCWG is a process that can replace conventional gasification and pyrolysis since water properties enable the production of a mixture of interesting syngases (mainly H_2, CH_4, CO and CO_2) from wet biomass at lower temperatures. The composition of the

obtained syngas depends on operating conditions that can be modulated to produce a gas that is rich in hydrogen [47].

Recently, several methods have been proposed for the manufacture of nanomaterials using supercritical fluids [48]. These processes, which exploit the properties of supercritical water and their flexibility, are generally more simplified and with less impact on the environment. As a result, nanomaterials with better performances have been produced [49]. The described applications of the use of sub and supercritical water are best illustrated by Figure 4 which shows the capabilities of this technology.

Overall, the hydrothermal oxidation process in supercritical water consists of four main steps: preparation of raw material for feeding and pressurization, reaction, formation and separation of salt, recovery of heat and finally depressurization [19].

3.1. SCWO Process

Figure 5 shows a schematic of the main stages of the supercritical or subcritical water oxidation.

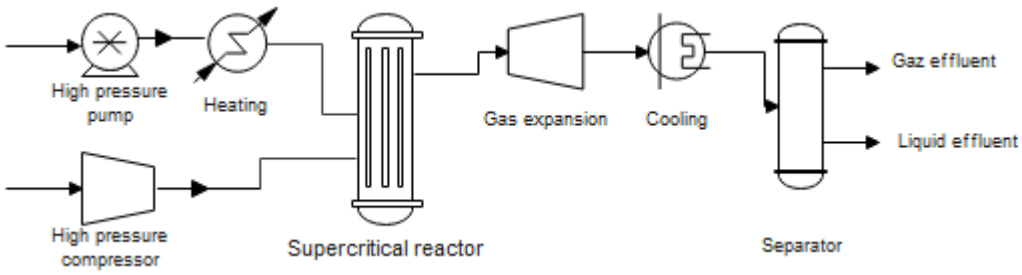

Figure 5. Schematic diagram of the SCWO (drawn using Superpro Designer software).

3.1.1. Preparation of Feed and Pressurization

The feed of a SCWO reactor is composed of the wastewater to be treated and an oxidant which can be pure oxygen, air, or hydrogen peroxide [50]. K. Hatakeda [51] studied the efficiency of hydrogen peroxide and oxygen on the oxidation of PBC in a temperature range of 473–723 K. The results showed that hydrogen peroxide was more efficient than pure oxygen. Usually, the wastewater is pressurized at more than 22.1 MPa and heated up above 374 °C. The oxidizer is fed at the same pressure and operating temperature and then added to the waste-water mixture [25,33]. Water and oxidant are mixed upstream of the reactor. S. Moussiere [22] diluted some of that waste before entering the reactor by means of an automatic valve to counterbalance the pressure drop created by the other valve placed on the water/oxidant line leading to the cold inlet of the reactor. This system allows water to be supplied with the waste in order to eliminate the pyrolysis phenomena of the organic compound that can occur in the injection tube in case the waste is injected pure or highly concentrated.

3.1.2. The Reaction

The feed streams of waste and oxidant mix in the reactor inlet, the oxidation reaction begins, and the organic compounds are oxidized by a rapid reaction [25,52]. At supercritical conditions ($P \geq 22.1$ MPa, $T \geq 374$ K), the organic compound, oxygen and water form a homogeneous single-phase mixture, facilitating complete and rapid reaction [25]. For the majority of waste, this state allows 99.99% elimination. However, the reaction in supercritical water can be done in a heterogeneous medium when the organic pollutant or the oxidation catalyst is solid [53]. As an example, obtaining reaction yields of the order of 99% for Ion Exchange Resins is very hard [54], even using a catalyst or a strong stoichiometric excess [55,56]. To overcome this problem, A. Leybros [54] has used isopropanol as a co-fuel to significantly improve the degradation yields of Ion Exchange Resins in supercritical water. Thus, the actual reaction schemes under supercritical conditions are much more complex and many intermediate products are formed; when the starting organic molecule

is complex [57], this reaction is highly exothermic [33,57] and the process becomes autothermal at only 3% of organic matter content in the effluent to be treated. From this concentration, excess energy can be used to generate electricity and heat [58].

3.1.3. Chemical Kinetics of the Oxidation Reaction

The mastery of reaction mechanisms is important to enhance the development of kinetic models necessary to design supercritical water reactors. If a detailed mechanism of reaction is not available, or if the wastewater is a complex mixture, a global model of reaction is needed. Nonetheless, global models can often be poor predictors outside of the specified experimental conditions [59].

The global reaction rate can be expressed as follows:

$$\text{Rate} = k\,(T)\cdot[\text{Pollutant}]^{a}\cdot[O_2]^{b}\cdot[H_2O]^{c} \quad (25)$$

where a, b, c are the kinetics reaction orders of pollutant, O_2 and H_2O, respectively, and k (T) is the reaction rate coefficient, which can be expressed in Arrhenius form as [60]:

$$k\,(T) = A\cdot\exp(-Ea/R\cdot T) \quad (26)$$

where Ea, is the activation energy and A is the pre-exponential factor.

In the last decade, there has been a growing interest in the organic reaction in water around its critical conditions, and several studies researched the oxidation mechanism in SCW in depth, taking into account the influence of water properties, and developing kinetics models have been advanced [19]. Li et al. [59] were based on a simple reaction scheme and proposed a global kinetics model for supercritical water oxidation of organic compounds. They examined that the kinetics of oxidation is controlled by the formation and elimination of intermediates: some organic compounds are directly converted into final oxidation products, whereas others are oxidized into stable intermediates.

Figure 6 shows the general reaction mechanism for the oxidation:

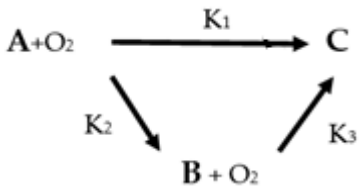

Figure 6. A two-stage oxidation mechanism according to Li et al. [59].

A, B and C are organic compounds and their respective concentrations (denoted as []) are defined as:

[A]: [all initial and intermediate organic compounds] − [acetic acid];

[B]: [Acetic acid];

[C]: [Final products of the oxidation].

It has been shown that this global kinetic model accurately predicts the evolution of both simple and complex waste experimental data of oxidation in sub- and supercritical water. It was satisfactorily used by Bermejo et al. [36] for isopropyl alcohol SCWO and also by S. Moussiere for Dodecane [22].

An adjustment of the above model was proposed by Portela et al. [61]; the reaction mechanism was divided into two ways: a direct oxidation and an intermediate oxidation of carbon monoxide, considered as a limiting step. The study was conducted at a temperature between 673 and 773 K and the proposed reaction scheme is shown in Figure 7 [61]:

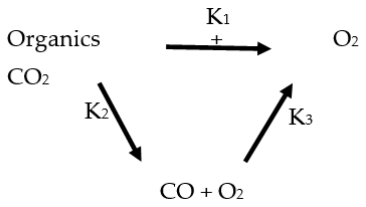

Figure 7. A two-stage oxidation mechanism according to Portela et al. [61].

This scheme has been used successfully to represent the oxidation kinetic of SCWO in the same study for cutting oils by J.R. Portela et al. [61], and also for the oxidation of methanol by Zhang et al. [62].

A kinetic model has been proposed by J. Sánchez Oneto et al. [63] for cutting fluids (Servol and Biocut) at a temperature between 400 °C and 500 °C and a pressure of 25 MPa. For the Servol, a kinetic model of pseudo-first order was used. In the case of the Biocut, a two-parameter mathematical model was used, since the reaction took place in two steps: a fast reaction followed by a slow one. This mechanism has been also used by Marulanda et al. [28] to model the SCWO oxidation of mineral transformer oil wastes which were very similar in composition to cutting oil wastes, and by Vadillo et al. [64] for the simulation of Biocut in the case of high concentrations. The same group of researchers has also proposed a global kinetic model for cutting fluids, in the same range of temperature and pressure of 25 MPa that was dependent on the oxygen concentration with a kinetic order of 0.58 [65]. This mechanism has been used successfully to model the SCWO oxidation of the "Biocut" cutting oil by J.M. Benjumea et al. [66].

Based on a global kinetic model for oxidation in supercritical water of methylamine proposed by Benjamin and Savage [50], Zhou et al. [67] developed a model for copper complex (Cu(II)-EDTA) SCWO at a temperature from 420 °C to 500 °C and a pressure of 25 MPa. CO_2 and CO were the main products including carbon and ammonia was the main intermediate nitrogen-containing.

It was determined that its oxidation was improved by the presence of copper in the complex. This mechanism has been successfully used by Zhou et al. [67] in their SCWO modeling study of the same component t-order reaction with respect to the organic compound [19]. Frequently, the kinetics of organic oxidation in supercritical water is supposed as a first order or pseudo first-order reaction with respect to the organic compound [19].

Several studies have performed kinetic studies based on the global reaction model to estimate kinetic parameters values for SCWO of several industrial wastewaters as shown in the below in Table 4. However, in addition to the global reaction kinetics, which simplified mechanisms and facilitate the development of SCWO simulation models with chemical reactions and the further design optimization of SCWO reactors, the detailed chemical kinetic models (DCKM) provide a detailed description of the chemical behavior of all molecular components and reaction intermediates. DCKMs are too complex to be coupled with flow and heat transfer equations to quantitatively describe a reacting flow [59].

Table 4. Kinetic parameters values for SCWO reaction of some organic pollutants.

Pollutant	T (°C)	P (MPa)	Ea (kJ/mol)	A ($(mol/l)^{1-a-b} \cdot s^{-1}$)	a	b	Ref.
Phenol	250–300	25	39.2 ± 10.7	$10^{1.34} \pm 0.77$	1	0	[68]
	250–300	25	39.6 ± 6	22 ± 9	1	0	[69]
	250–300	25	80 ± 30	$4.2 \pm 1.1 \times 10^3$	1	0	[69]
Methanol	454–563	24.6	97.7 ± 20.4	$10^{26.2 \pm 5.8}$	1	0	[70]
	400–500	25	203 ± 30	$6.7 \pm 1.2 \times 10^{12}$	1	0	[69]
	500–550	25	125,000	10^6	1	0	[25]
	427–485	27	200,617	2.951×10^{13}	1	0	[69]

Table 4. *Cont.*

Pollutant	T (°C)	P (MPa)	Ea (kJ/mol)	A ((mol/l)$^{1-a-b}$·s^{-1})	a	b	Ref.
Acetic Acid	400–500	25	149 ± 20	$1.5 \pm 0.2 \times 10^9$	1	0	[69]
	490–600	25	170	10^7	1	0	[71]
	350–700	23	172.2 ± 1.7	$(9.3 \pm 0.7) \times 10^{10}$	0.89 ± 0.07	0.2 ± 0.1	[72]
Ethanol	260–350	25	53.8 ± 4.6	$10^{2.9 \pm 0.4}$	1	0	[73]
	430–490	10	166.5 ± 6.1	$10^{11.6 \pm 0.4}$	1	0	[74]
Oily sludge	390–450	23–27	213.13 ± 1.33	8.99×10^{14}	1.405	0	[74]
Oil olive mill	380–500	25	35	15–30	1	0	[75]
	200–325	30	48 ± 13	140 ± 90	1	0.15	[76]
	400–650	10–30	0.214 ± (0.5)	33.24 ± 0.09	1.02 ± 0.031	0.89 ± 0.054	[77]
Isopropyl amine	411–618	25	64.12 ± 1.94	$(2.46 \pm 0.65) \times 10^3$	1.13 ± 0.02	0.24 ± 0.01	[78]
Ammonia	655–704	13.6–27	83 ± 19	$10^{19 \pm 4.5}$	1	0.44 ± 0.3	[79]
Cutting oil "servol"	400–500	25	79.80	1.111×10^5	1	0	[63]
Cutting oil "Biocut"	40–500	25	62.20	3207	1	0	[63]
			86.70	13,020	1	0	
Cutting oil	400–500	25	70	35	1	0.58	[65]

T: Temperature; P: prT: Temperature; P: Pressure; Ea: Activation Energy (kJ/mol); A: The preexponential factor ((mol/l)$^{1-a-b}$·s^{-1}), a and b are the partial orders of the pollutant and O_2.

In 1991, Li et al. developed a kinetic model for wet oxidation (WO) of organic compounds based on a simplified reaction scheme considering acetic acid as the rate-limiting intermediate as shown in Figure 8. This was validated for a variety of organic compounds, wastewaters and sludges in both subcritical and supercritical water oxidation processes [59].

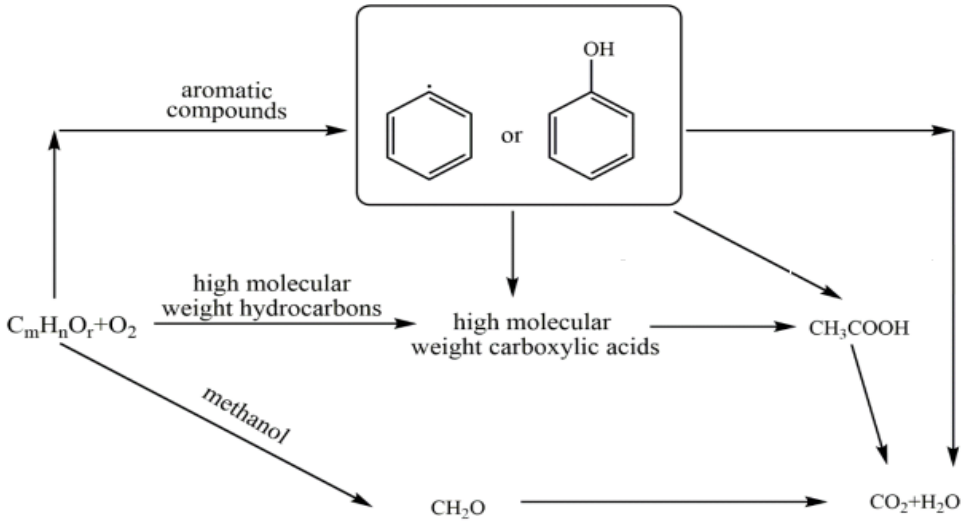

Figure 8. The simplified reaction network for hydrocarbon oxidation in SCW [59].

Recently, Ashraful and da Silva developed a detailed chemical kinetic model for supercritical water oxidation of methylamine (CH_3NH_2), providing insight into the intermediates and final products formed in this process as well as the dominant reaction pathways. The model was adapted from previous mechanisms with a revision of the peroxyl radical chemistry to include imine formation, which has recently been identified

as the dominant gas-phase pathway in amine oxidation. The model is described by the following equation [80]:

$$CH_2NH_2 \overset{+O_2}{\rightarrow} CH_2NH \overset{+H_2O}{\rightarrow} [NH_3 + CH_2O] \quad (27)$$

3.1.4. Formation and Separation of Salts

Due to the properties of water at the supercritical state, organic substances and oxygen have complete solubility, whereas species with high polarity, such as inorganic salts, are insoluble and precipitate [17]; this phenomenon is caused by the low dielectric constant of the supercritical water and depends on how well the reactor sealing is ensured [54]. Organic heteroatoms such as chlorine, sulfur, phosphorus, are transformed to their corresponding mineral acids (HCl, H_2SO_4, H_3 PO_4) which may be neutralized with a base and precipitate [20,21].

Salt precipitation on the internal surface of the equipment increases resistance and degrade the heat transfer efficiency. It may cause an increase in resistance to heat transfer and degrade its efficiency. This can lead to corrosion damage to the reactor, blockages in the tubes and pipes causing shutdowns of the installations to avoid explosions [52].

Thereby, corrosion of equipment in supercritical water oxidation (SCWO) installation, is one of the principle obstacles to the commercialization of the SCWO process [81] and the transition of the process to an industrial scale application [82] despite the observed treatment efficiencies.

3.1.5. Cooling and Heat Recovery

At the outlet of the reactor, the products are at high temperature and high pressure depending on the reactor design and the heat of the reaction or nature of pollutant. As an example, in the work of M.D. Bermejo et al. [83], the SCWO of coal, led to outlet stream of 650 °C and 30 MPa. Therefore, the outlet stream must be cooled and depressurized; which leads to a reuse of the residual heat to preheat the input effluents up to the operating temperature and also to recover the energy from the depressurization. At the end, the flow is separated into a liquid phase and a gas phase in a gas/liquid separator [84].

Depressurization of the effluent process is a key aspect in SCWO plants because proper operation involves an adequate control of the system pressure. Thus selection of the best pressure control system is crucial in the design of SCWO plants [83].

As a result, several propositions of energy recovery form SCWO processes were proposed in the literature [10,11,16,19].

4. Supercritical Water Oxidation Reactor

The reactor is truly the heart of the hydrothermal oxidation process, the technological developments of hydrothermal oxidation in supercritical water reactors have been aimed at optimizing heat transfer (exothermic reaction) and dealing with problems of precipitation of salts due to operating conditions in pressure temperature, and problem of corrosion [54]. A variety of designs for reactors have been developed to solve these problems. In what follows, we will cite the most used. Existing reactor concepts can be classified into two main categories: tubular and tank reactors. The tubular reactor has some advantages, since it is easily implemented by simple commercially available tube soldering; it is well suited to high pressure because of its high-rise area compared to its volume, it is also possible to control the residence time of the effluent and thus its conversion rate [85].

In the case of tank reactors, it is hard to obtain a homogeneous concentration at the interior of the reactor as well as uniform residence times (presence of dead volume) [85]. One of the first SCWO reactors developed was the Modar tank type, which was used to create the Modar process by Modar Inc in the 1980s. This reactor is divided into two zones, a supercritical upper zone and a subcritical lower zone, as shown in Figure 9. The principle consists in injecting the supply of aqueous solution into the upper zone of the oxidation reaction and the inorganic salts precipitate and fall by gravity into the lower zone where

they are re-solubilized and evacuated [86]. However, the temperature gradient between the top and bottom of the reactor causes high heat loss, and the energy produced by the reaction is not recoverable. In addition, recovery of salts continuously is difficult. The brine produced is highly corrosive and rapidly accumulates at the bottom of the reactor [22].

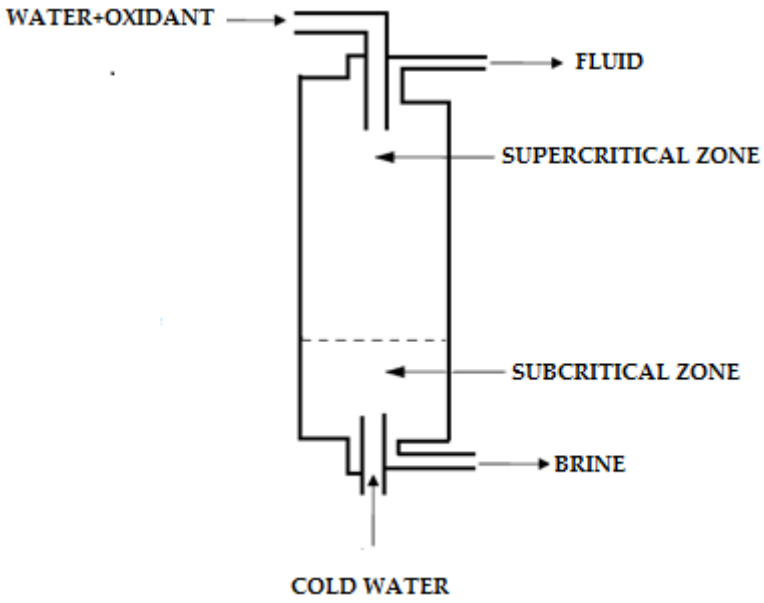

Figure 9. Modar SCWO tank type reactor [86].

Concerning the category of porous wall reactor, Summit Research Corp. Ref. [32] developed a Transpiring Wall Reactor (TWR) for Supercritical Water Oxidation processes in the interest of reducing corrosion problems and overcoming salt deposition. Figure 10 shows their TWR which comprised a reaction vessel encircled by a cooling water wall that formed a protective film in opposition to salt deposition and corrosive agents. This type of reactor is two concentric tubes; the waste and the oxidant are injected into the inner tube, while cool water flows between the reactor external wall and the porous wall [36]. In this reactor the addition of water to the reaction zone results in a dilution of waste.

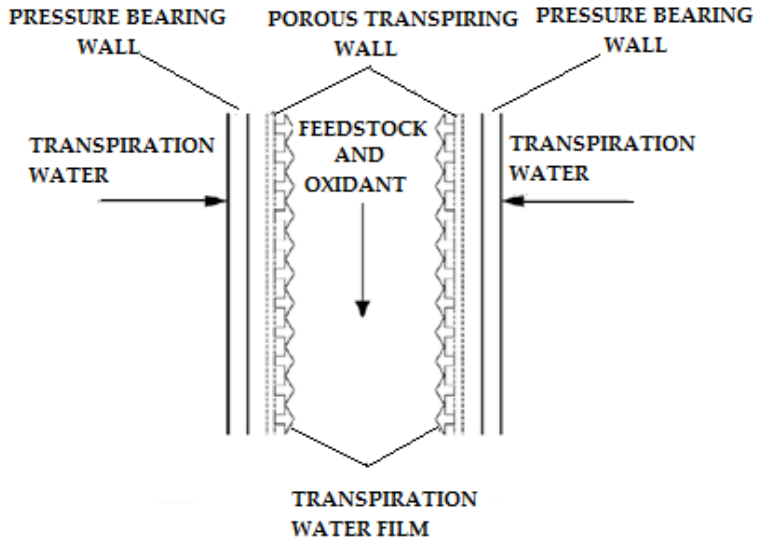

Figure 10. Transpiring wall porous reactor [36].

The tubular reactor is particularly well suited for achieving the short residence times required by hydrothermal oxidation using high flow rates. Modec patented a process based

on extremely high fluid velocities, with an inner diameter of 6.6 mm, because the small diameter makes the reactor particularly sensitive to the problem of solid deposits and clogging. This reactor contained a brush inside the reactor, to scrape the inner walls of the tube between two operating periods. However, high fluid velocities involved very long reactor lengths to achieve residence times greater than one minute [85].

The Chematur process (Japan) reactor shown in Figure 11 was developed for the purpose of regulating the exothermic (heat) of the reaction. The principle is shown in the following figure:

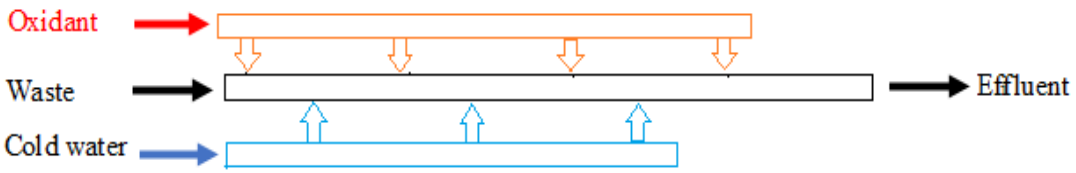

Figure 11. Tubular Chematur type reactor [85].

The waste in this reactor may be oxidized in more than one stage, first the wastewater and the oxidant are introduced, and once the oxidant is completely exhausted and the temperature reached the 600 °C, a stream of cold water is added to reduce the temperature to about 400 ° C. Then, a new injection of oxidant is conducted. This regulation is continued throughout the reactor until the organic charge is completely destroyed [59]; this multi-injection of water causes shocks and thermal fatigue at various points of the reactor. In addition, the consumption of cooling water is important and involves dilution of the effluent [85]. A reactor of this type has also been developed on a semi-industrial scale by the Hydrothermal Oxidation Option (HOO) [52].

Another reactor, also developed in the Institute of Condensed Matter Chemistry of Bordeaux ICMCB [87] to control the exothermic of reaction and thus treat a larger quantity of waste, is tubular with a multi-injection of oxygen (3 points), as shown in Figure 12:

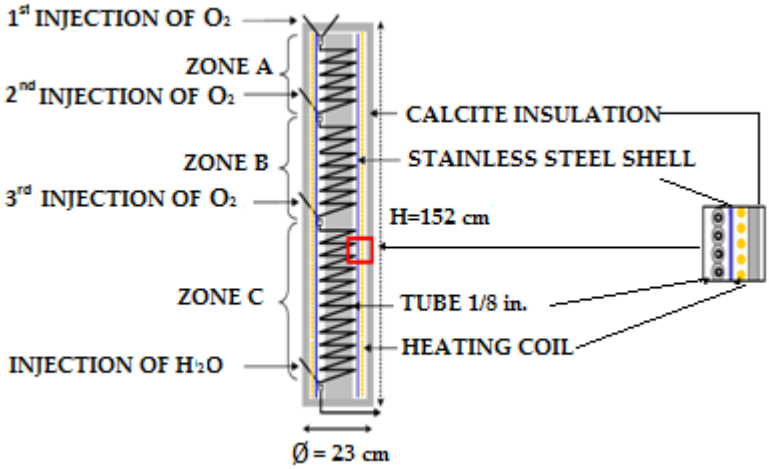

Figure 12. Vertical multi-injection reactor [87].

A cooled-wall reactor has been developed at the Department of Chemical Engineering at the University of Valladolid in Spain and shown in Figure 13 as [52]:

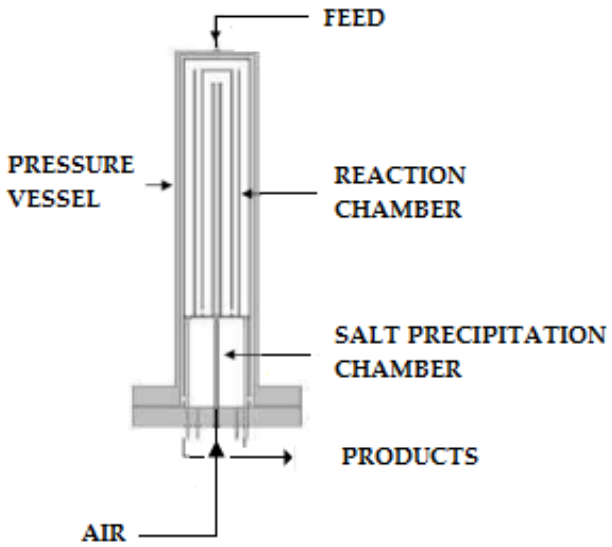

Figure 13. Cooled wall SCWO reactor [52].

The temperature and pressure effects are isolated in this type of reactor. This is accomplished by using a cooled-walled tube, which is held at almost 400 °C. The reaction vessel is made of a particular material resistant to the oxidant environment of the reagents at a high temperature of 800 °C and a pressure of 25 MPa. It is encircled in the main tank, which is pressurized and cooled down with the feed stream before reaching the reaction vessel, so that it runs at around 400 °C and does not have an oxidizing atmosphere. Hence, this pressure chamber can be made of stainless steel [52].

In 2005, the Supercritical Fluids Laboratory of the University of Cádiz in Spain developed an experimental SCWO reactor at a pilot scale 2005 [66], as shown in Figure 14:

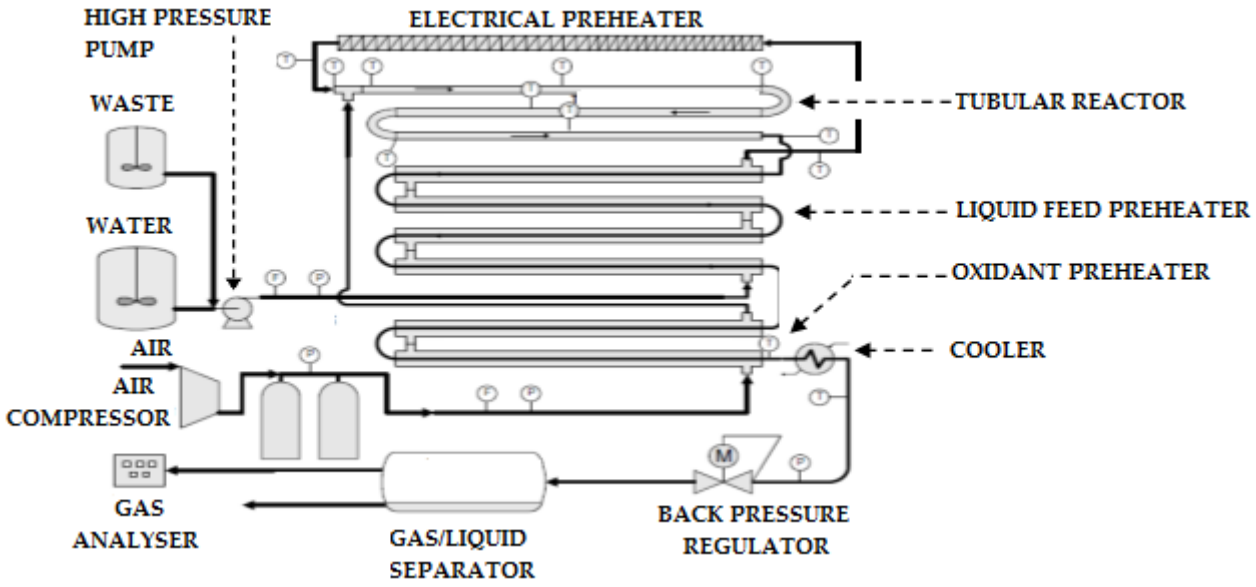

Figure 14. Pilot SCWO reactor [66].

The tubular reactor was made of stainless steel 316L with a specific 3.365 mm wall thickness of a tube to boost its pressure resistance, an inner diameter of 12.32 mm, and a total reactor volume of 1229.553 cm^3. The temperature of the streams at the reactor inlet is around 420 °C and can be increased up to 550 °C at its outlet.

Firstly, the effluent and air are pressurized separately up to 250 bars and then the two streams are heated to reach a temperature around 420 °C for the effluent stream and 200 °C for air. To measure the temperature profile produced in the reaction system, thermocouples are installed along the reactor. At the end, the product stream is cooled and depressurized by a back pressure regulator and then split into two phases in a gas/liquid separator.

This pilot plant has been successfully used for several previous studies in SCWO for the destruction of many pollutants (phenol [20], cutting oil [2,5,14], flammable industrial wastewaters [3]). Initially, this reactor was used with a single injection of oxygen and to enhance the efficiency of the oxidation of the supercritical water, in particular the efficiency of the destruction of the pollutants and the mastering of the temperature in the reactor, separate cooling water injectors and oxidizers were installed [88]. Due to the use of cooling water and a different distribution of air between the two injectors, it is possible to treat a greater concentration of feed while keeping the temperature under control.

To overcome the corrosion problems, a double shell reactor has been advanced in the laboratory of supercritical fluids and membranes of the CEA «Central commission of nuclear energy» Pierrelatte in France [89], as shown in Figure 15:

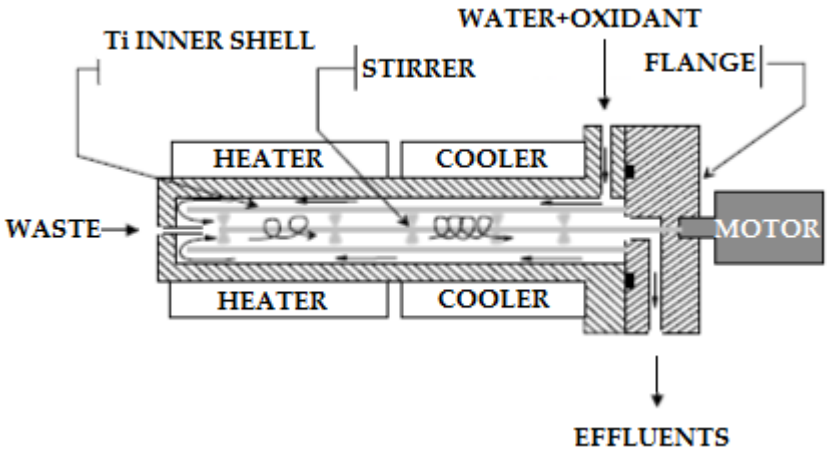

Figure 15. Double shell reactor [68].

This reactor has, in addition to a jacket made with titanium to prevent corrosion, an agitator creating a turbulent flow, preventing precipitation of the inorganic compounds; and allowing better heat transfer. It was very useful for the oxidation of organic compounds containing salt. Consequently, after several uses for long periods of time, no macroscopic evidence of corrosion could be found inside a double shell. In addition, the stirring rate is used to monitor the temperature evolution of fluids and, in particular, one of the exit effluents [89].

Figure 16 shows a novel reactor was designed in China by combining the benefits of Modar reactor and transpiring wall reactor in order to resolve the two main difficulties: reactor plugging and corrosion. The mixing of oxidant and preheated sewage sludge was achieved by a specially designed mixer mounted on the pipe line of the reactor inlet, the central pipe is placed deep into the reactor and the diameter is wide enough to avoid plugging. Heating the reactants inside the pipe was accelerated by high temperature fluids around or by reaction heat produced by partial oxidation. In this reactor, the top cover is cooled by low-temperature water in a vessel shaped between the top cover and the cooling cover. Low temperature water is transferred from two pores to the top of the chamber, and then enters the upper annular space between the transpiring wall and the pressure-bearing wall to be used as transpiration water [90].

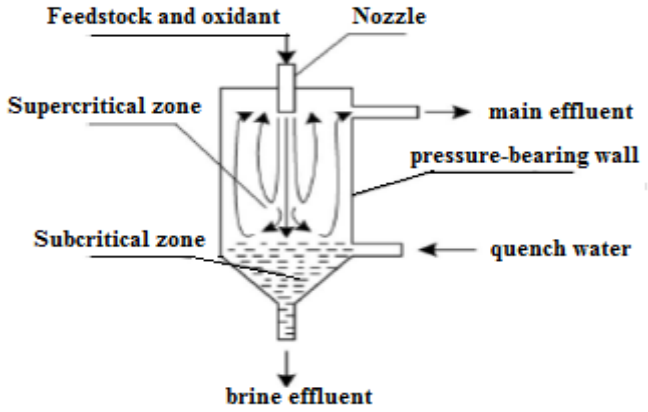

Figure 16. Reverse flow tank reactor [90].

Another novel reactor was designed also in China [91], and it combined the advantages of the MODAR reactor, horizontal stirred reactor, dynamic gas seal wall, and cool wall reactor. It was performed and designed to avoid the previous difficulties encountered when oxidating real waste in continuous supercritical water, particularly in the semi-solid state. This reactor had a Y shape with two sections separated by an angle of 70°. The left section is a three-wall reactor including an outer pressure-bearing wall, a middle distribution wall, and an inner porous wall. The distribution internal diameter was 46 mm and four holes are located on the underside of the nonporous distribution wall. Figure 17 illustrates this type as:

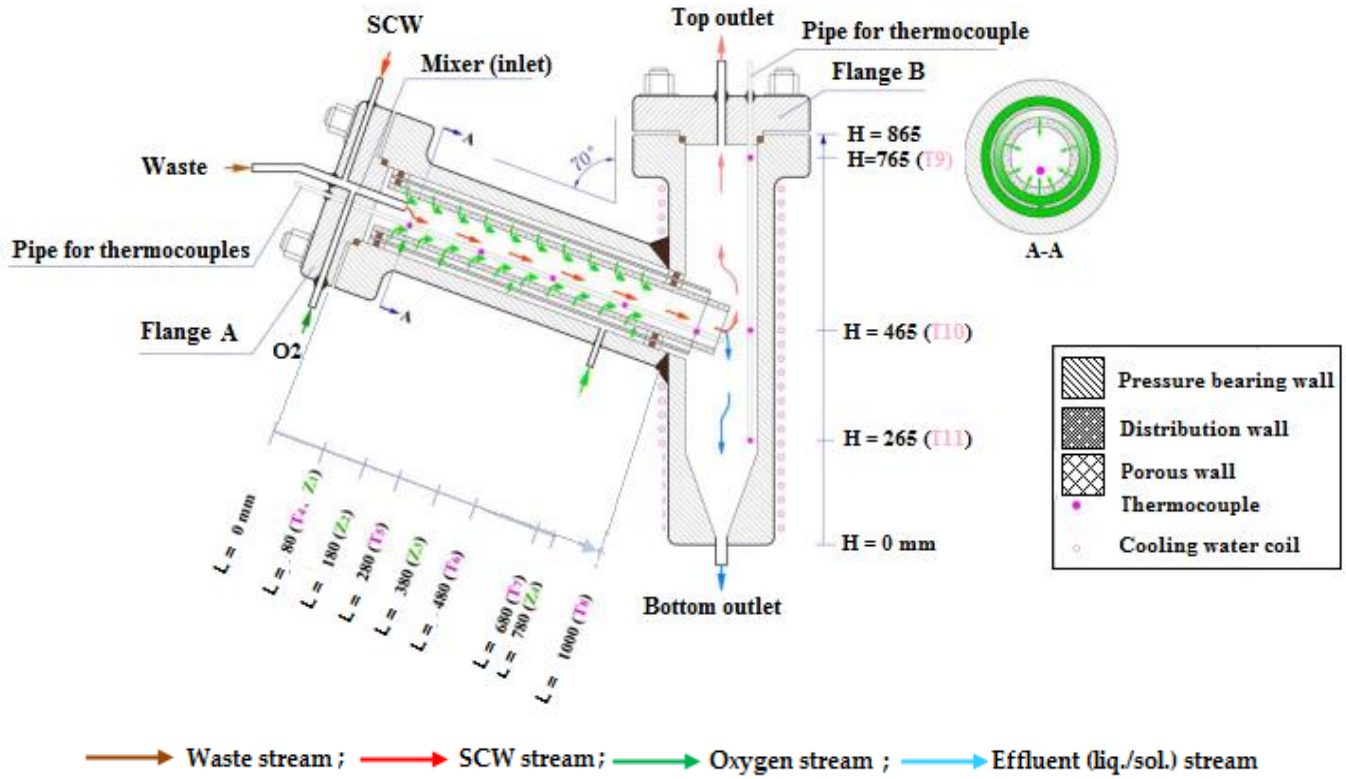

Figure 17. Scheme of the 'Y' shape reactor [91].

The porous wall was built of sintered wire mesh formed with 20 layers of 316 L stainless steel nets with a pore size of 5 μm; its internal and external diameters were 35 mm and 40 mm, respectively. For maximum operating conditions of high pressure

and temperature (32 MPa and 600 °C), a pressure bearing wall with internal diameter of 60 mm was designed. Air is introduced into the reactor through the sole inlet on the side of the pressure-bearing wall. In addition to its role as an oxidant, air plays the role of a transpiring fluid to prevent the deposition of salts and corrosion of the porous wall. Moreover, an independent additional line for pure oxygen (O_2) is added as the principal source of oxidant.

The reactor's left and right sections were fitted with two independent electric heating with a maximum power of 6 kW each. The heat exchangers were designed to provide start-up heat and maintain reactor temperature during the experiments. The left part is the area of reaction, and the right part is the area of separation; there is no interaction between the two zones [91].

Finally a comparison of the advantages and disadvantages of the different described reactors is shown in Table 5 as:

Table 5. Comparison of advantages and disadvantages of the described reactors.

Reactor Type	Figure	Main Advantages	Main Disadvantages
Modar SCWO tank type reactor [86]	Figure 9	- Easy implementation by simple available tube soldering; - Suitable for high pressure due to high-rise area compared to volume; - Control of the residence time of the effluent and its conversion rate.	- High heat losses due to the temperature gradient between the top and bottom of the reactor; - A Difficult continuous salts recovery; - Highly corrosive brine, accumulating at the bottom of the reactor
Transpiring Wall Reactor (TWR) [36]	Figure 10	- Reduced corrosion problems, overcoming salt deposition; - Achieved short residence times required by hydrothermal oxidation using high flow rates	- Dilution of the hot reaction products by mixing with the transpiring water; - Less efficient heat recovery due to reduced reactor effluent temperature.
Tubular Chematur type reactor [85]	Figure 11	- Particularly sensitive to the problem of solid deposits and clogging, due to very high fluid velocities;	- Important Length to achieve residence times greater than one minute due to involved high fluid velocities.
Vertical multi-injection reactor [87]	Figure 12	- Good control of the exothermic heat of reaction and thus treat a larger quantity of waste; - Tubular reactor with multi-injections of oxygen	
Cooled-wall reactor [52]	Figure 13	- Isolated temperature and pressure effects allow feed preheating inside the reactor, hence a compact unit very appropriate for mobile units.	- Low energy recovery; - Cooling of hot products and dilution by mixing with the transpiring cold water; - Plugging problems when the salts would not exit the reactor in a water solution; - Outlet temperature not under the critical point of water, hence low salt solubility and heat recovery.

Table 5. *Cont.*

Reactor Type	Figure	Main Advantages	Main Disadvantages
Cadiz SCWO pilot scale reactor [66]	Figure 14	- Successful use in SCWO for the destruction of many different nature pollutants; - SCWO efficiency enhanced with a single injection of oxygen, hence an efficient destruction of the pollutants; - Treatment of a greater feed concentration with temperature control, using cooling water and a different distribution of air between the two injectors	- The use of air as oxidant, has a great effect on the behavior and performance of the reactor. - More energy is required for the heating up of air stream to the temperature of the main stream (400 °C).
A double shell reactor [68]	Figure 15	- Resistant to corrosion by means of a titanium jacket; - Prevention of inorganic compounds generation by promoting turbulent flow, hence better heat transfer; - Efficient oxidation of organic compounds; - No macroscopic evidence of corrosion inside a double shell, after several long time uses; - Monitoring of the temperature evolution of fluids, particularly the exit effluents, by means of an adequate stirring rate.	- Char formation during oxidation, due to imperfect mixing between the pure organic and the aqueous oxidative phases.
Reverse flow tank reactor [90]	Figure 16	- Reactor plugging and corrosion resolved; - Plugging avoided with a wide enough diameter; - The mixing of oxidant and preheated sewage sludge achieved by a specially designed mixer mounted on the inlet pipe line of the reactor; - Acceleration of reactants heating inside the pipe by high temperature fluids around or by reaction heat produced by partial oxidation.	- Salt deposition on the reactor internal surface due to low falling velocity of small particle; - Great quantities of energy required to preheat the transpiration water entering into reactor.
'Y' shape reactor [91]	Figure 17	- Avoid the previous difficulties encountered when oxidating real waste in continuous supercritical water, particularly in the semi-solid state; - Great potential for application in hydrothermal processes involving high content of inorganic solid particles; - Destruction of great varieties of organic wastes where conventional methods failed.	- Important corrosion and plugging during preheating, particularly with high organic, salt and solid composition; - Complex effluents may cause plugging of units like heat exchanger, cooler, line pipes, and back-pressure valve.

Further progress and advancement in SCWO reactor technology and design are needed in reactor corrosion control, reliability improvement, and reaction efficiency improvement, maintenance and security ease.

5. CFD Modeling of SCWO Reactor

Due to the high cost of the construction and operation of these reactors, the development of simulations is of great interest [19]. The modeling of hydrothermal oxidation in supercritical water has been the subject of several research studies on different types of reactors and different types of pollutants with different turbulence models. Most often,

these studies used commercial CFD (Computational Fluid Dynamics) software to solve mathematical models and get the temperature profiles and concentrations along the studied reactor. Also, several studies were interested in developing reliable correlations to estimate the coefficient of heat transfer for reactors in supercritical medium, as well as studies on the possibilities of energy recovery of the processes. The objective of the modeling is a better understanding of the process: optimization of its operating conditions, design and scale-up to an industrial scale.

The development of processes is based on recent advances in kinetic models, reactor technology and experimental operating conditions, depending on the research and development of simulation tools, which enable the researcher not only to understand the complex multiphysical phenomena that characterize the system but also to optimize the operating factors in order to reach the best performance of the process and ensure its safe operation [28].

These models are based on conservation of mass, momentum, energy and the variation of the different species, and, also, simplifying the hypotheses relating to the properties of the reaction medium, thermal losses, the estimation of the coefficient of heat transfer and particularly the flow regime in the reactor.

As the reaction mixture comprising more than 70% of water, Fourcault et al. [33], Marias et al. [92], Serin et al. [42] and Withag et al. [41] considered that the physical and thermodynamic properties of the medium are considered those of pure water and used the IAPWS formulation for their estimation.

The most important step in supercritical reactor modeling is chemistry and transfers, the description of phenomena and mechanisms falls into the following three areas:

5.1. The Hydrodynamics

The flow rate in supercritical water reactors depends on the geometry [22], and the modeling of the hydrodynamics of a flow is built using the mathematical formulation of the conservation of mass, momentum and energy.

- Conservation of Mass

$$\frac{\partial \rho}{\partial t} + \nabla \cdot \left(\rho \cdot \vec{u} \right) = 0 \tag{28}$$

With: ρ: the density (kg/m^3) and $\vec{u}$: the velocity vector (m/s).

- Conservation of Momentum

$$\frac{\partial \left(\rho \cdot \vec{u} \right)}{\partial t} + \nabla \cdot \left(\rho \cdot \vec{u} \cdot \vec{u} \right) = -\nabla P + \nabla \cdot \left(\bar{\bar{\tau}} \right) + \rho \cdot \vec{g} + \vec{F} \tag{29}$$

With: P: pressure (kg·m/s^2 or Pa), $\vec{g}$: gravitational forces (kg·m/s^2), $\vec{F}$: all external forces.

The stress tensor $\bar{\bar{\tau}}$ expresses the tensor of the viscous stresses and is given by the following relation:

$$\bar{\bar{\tau}} = \mu \cdot \left[\left(\nabla \vec{F} + \nabla \vec{u}^{T} \right) - \frac{2}{3} \nabla \cdot \vec{u} \, I \right] \tag{30}$$

With: μ the viscosity (kg/m·s) and I: the unit tensor [93]. We can write for a direction i [94–96]:

$$\tau_{ij} = \mu_{eff} \left[\left(\frac{\partial u_i}{\partial x_j} + \frac{\partial u_j}{\partial x_i} \right) - \frac{2}{3} \frac{\partial u_k}{\partial x_k} \delta_{ij} \right] \tag{31}$$

τ_{ij}: the viscous stress tensor (i, j, k = 1, 2, 3)
μ_{eff}: the effective viscosity (kg/m·s).
δ_{ij}: is the delta function Kronecker (δ_{ij} = 1 s_i i = j et δ_{ij} = 0 s_i i $\neq$ j).

u_i, u_j, u_k: represent the three components of the velocity $\vec{u}$.

For a turbulent flow, $\mu_{eff} = \mu + \mu_T$ where μ_T is the turbulent viscosity. The latter is defined using an appropriate turbulence model [97] and the most commonly used in hydrothermal oxidation modeling are k-ω and k-ε models. The model numerical resolution is often done using CFD simulators such as Fluent [26,98], Comsol [28,41] and ProsimPlus [99].

In the case of a turbulent flow, it is imperative to solve these equations on small cells in order to correctly represent all scales of the turbulence, turbulence transport equations are also added in the model.

Fourcault et al. [33], S. Vielcazals et al. [35] assumed that the stress tensor equals the linear local pressure drop inside the reactor to facilitate calculations, and next they [35] developed a mathematical model based on one-dimensional geometry for any organic compound in an oxidation reactor in supercritical water. The reactor was horizontal and tubular with multi-injection points of oxidant (3 points) to control the exothermic heat of the reaction and to treat a larger quantity of waste. The results of this model have been compared to data of experimental works of ICMCB, in the case of supercritical oxidation of methanol [35], acetic acid and phenol [33,34]. Nevertheless, this model provides a good estimate of the temperature profile along the reactor and given an indication of the heat to be recovered.

5.2. Conservation of Species

As we mentioned, the detailed description of the reaction mechanism includes a large number of intermediate species; however, for reasons of mathematical simplification, the reaction can be represented by the following equation where the oxidant is oxygen [33,35,100]:

$$C_\alpha H_\beta O_\gamma N_\Psi + (\alpha + \beta/4 - \gamma/2)\, O_2 \qquad \alpha CO_2 + \beta/2\, H_2O + \Psi/2\, N_2 \tag{32}$$

In the general case, the species conservation equation is:

$$\frac{\partial}{\partial t}\left(\rho y_j\right) + \nabla\cdot\left(\rho\cdot\vec{u}\cdot y_j\right) = -\nabla\cdot\vec{J_j} + R_j + S_j \tag{33}$$

With: $\vec{J_j}$: the flow of diffusion of species, y_j: the mass fraction of species j, R_j: the net production rate of species j by chemical reaction, S_j: is a source term that includes the energy provided by the chemical reaction [93].

5.3. The Heat Transfer

Heat transfer in hydrothermal oxidation reactors can occur by conduction (between the reactor material and the external medium), as long as there is a thermal gradient in a material medium; and by convection, in the reaction flow medium. The global equation of the energy balance is written according to the equation:

$$\frac{\partial}{\partial t}(\rho\cdot E) + \nabla\left(\rho\cdot E\cdot\vec{u}\right) = -\nabla\cdot q - \nabla\left(P\cdot\vec{u}\right) + \dot{Q} - \nabla(\bar{\bar{\tau}}\cdot\vec{u}) \tag{34}$$

where: $E = h - P/\rho$, q: the total heat flux exchanged defines by a convective flux due to the diffusion of the species.

$\dot{Q}$: Heat source, which includes the energy provided by the chemical reaction.

The expression of the reaction rate depends on the operating mode. In the case where the chemical reaction is sufficiently slow compared with the transport phenomena (chemical regime), the reaction rate is determined from the kinetics of the reactions, and the Arrhenius law is used. If the chemical reaction is very fast in hydrodynamic processes, the mixing step may become limiting and it is necessary to take into account the influence of turbulence on the local concentrations of the species "reactive flow". In this context it is necessary to use appropriate models like: finite rate, or Eddy dissipation [22,54].

Moussiere et al. [26] allowed setting up and validating a model based on bidimensional geometry for the reactive monophasic flow, in a stirred double shell reactor, for dodecane, they have been chosen two approaches to predict the oxidation reaction rate. Firstly, the reaction rate is estimated using the Arrhenius law and secondly using the Eddy Dissipation Concept (EDC) model that considers the chemistry-turbulence interactions. The study of this reactive flow showed that the temperature predictions were better for the EDC model yielded correct temperature profiles, indicating that the rate of reaction is controlled by the mixture of species. Nevertheless, an overestimation of the temperature when the thermal gradients are important has been observed.

In this same reactor of Moussiere et al. [26] and to be able to master the influence of the particles on the dynamics of the flow, as well as the transfer of matter in the proximity of the reactive particles, Leybros et al. [101] studied the simulation of biphasic reactive turbulent flow on 2D axisymmetric geometry for the degradation of IER «Ion Exchange Resins»; the rate of reaction is controlled by the mixture of species, and the Eddy Dissipation Concept is therefore used to model the process. The results of this modeling provide an indication on the degradation of IER products (hydroxybenzoic acid, phenol and acetic acid) and CO_2 formation. This simulation shows that the reactive zone is mostly detected in the stirrer top; where particles solubilization took place and as a result hydroxybenzoic acid is produced. The obtained temperature profile showed a higher temperature zone (close to 1200 K).

V. Marulanda et al. [28] used the k-epsilon turbulence model (k-ε) under the CFD Comsol Multiphysics 3.3 simulator, with a bidimensional representation, where the properties of the reaction medium were supposed to be that of pure water. The objective of the proposed model was to reach the optimal operating conditions and achieve a more reliable pilot operation where the reactor was tubular and the mineral transformer oil heavily contaminated with PCBs to be removed with hydrogen peroxide as an oxidizing agent. The model results showed that the operation of the suggested pilot was not possible; due to the high temperature caused by the exothermic oxidation reactions, it increases up to 1000 K for an inlet temperature equal to 800 K. It is then appropriate to use a lower inlet temperature in order to avoid hazardous operating temperature conditions, while maintaining the objectives of destroying organic charge and identical PCBs.

A 3D model of continuous stirred tank reactor has been applied by Zhou et al. [102] to simulate the SCWO of methanol; they used the turbulence model k-ε at low Reynolds numbers. The simulations demonstrated phenomena of non-ideality of the mixture in the reaction; these may include short circuits to the power supply. The simulation showed that the measured conversion rates varied slightly, depending on the position of the system sampling.

All of these studies were conducted in a stationary state; the modeling of a SCW reactor in a transient and time-dependent state has scarcely been considered in the literature. This is, in all probability, due to the adversity generated by the two difficulties: the rapid variation of temperature and the radical difference in the properties of the substances around the critical point, which stem from problems of convergence and stability.

Benjumea et al. [67] developed a one-dimensional mathematical model under Mathlab simulation software, for the tubular reactor developed at the University of Cádiz, it was based on mass conservation, energy and momentum equation, and the variation of the different species, in a transient state. The objective of the study was to better understand the time-dependent performance of the SCWO process. Simulations results were compared to experimental temperature profiles for cutting oils and gave a good agreement. This model showed the effect of time variation on process operating conditions behavior such as temperature, species concentration or heat losses along the reactor.

Heat Transfer Coefficient for SCWO Reactors

The estimation of the heat transfer coefficient to quantify the heat transfer between the reactor and the external environment is an important step in the modeling of supercritical reactors. The main factors influencing the coefficient of heat transfer values are

the temperature and the total flow rate according to previous works. Fourcault et al. [33], used blank experiments to estimate the heat transfer coefficients, which means experiments without pollutant and only with pure water and oxidant as inlet streams of the reactor, in the absence of chemical reaction.

Belén Garcia Jarana et al. [99] estimated the heat transfer coefficient using experimental temperature profiles and process simulation using PROSIM PLUS 2.1 software. Using temperature profiles resulting from different blank experiments, an empirical equation was suggested in terms of total flow rate and temperature for the estimation of the heat transfer coefficient.

For heat transfer analysis at sub and supercritical state, there is much published research devoted to the subject, in particular to estimate the heat transfer coefficient and other parameters under supercritical conditions, which has been used much more in the field of "supercritical water cooled nuclear reactor" (SCWR) [103,104].

Several equations were proposed to estimate the internal heat transfer coefficient in SCWR and the most commonly used one at subcritical pressures for forced convection was the Dittus–Boelter correlation (1930), McAdams (1942) [103]:

$$Nu = 0.0243 \times Reb^{0.8} \times Prb^{0.4} \quad (35)$$

Equation (35) was also used at supercritical conditions.

The majority of the empirical correlations proposed have a modified Dittus and Boelter equation in its general form as shown in the following [105]:

$$Nu_x = C \cdot Re_X^m Pr_m^n \cdot F \quad (36)$$

The correction factor F that takes into account fluids properties variation and reactor geometry; thus, F is a function of (ρ_w/ρ_b, Cp_w/Cp_b, k_w/k_b, μ_w/μ_b and L/D). With:

ρ_w, Cp_w, k_w and μ_w: Density (kg/m^3), heat capacity (J/kg·K), conductivity (W/m·K) and viscosity (Pa·s) of fluid at wall temperature, respectively.

ρ_b, Cp_b, k_b and μ_b: Density, heat capacity, conductivity and viscosity of fluid at bulk temperature respectively.

L: the length of the reactor and D: the inner diameter.

Table 6 shows some correlations with other derivatives for heat transfer coefficient in supercritical reactor under different conditions of temperature, pressure, mass flow and heat flow in a circular tube.

Table 6. Selected correlations for heat transfer in supercritical reactors [103,106].

T (°C)	T (MPa)	Mass Flux (kg/m^2·s)	Heat Flux (MW/m^2)	Correlation
282–527	22.6–27.5	651–3662	0.31–3.46	$Nu_b = 0.0069 Re_b^{0.9} Pr_b^{0.66} \cdot \left(\frac{\rho_w}{\rho_b}\right)^{0.43} \left(1 + 2.4 \cdot \frac{D}{L}\right)$
75–576	22.8–41.4	542–2150	/	$Nu_w = 0.00459 Re_w^{0.923} \overline{Pr}_w^{0.613} \cdot \left(\frac{\rho_w}{\rho_b}\right)^{0.231}$
/	/	/	/	$Nu_b = 0.0183 Re_b^{0.82} Pr_b^{0.5} \cdot \left(\frac{\rho_w}{\rho_b}\right)^{0.3} \cdot \left(\frac{\overline{Cp}}{Cp_b}\right)^n$
/	23–30	600–1200	0.1–0.6	$Nu_b = 0.02269 Re_b^{0.8079} \overline{Pr}_b^{0.9213} \cdot \left(\frac{\rho_w}{\rho_b}\right)^{0.6638} \cdot \left(\frac{\mu_w}{\mu_b}\right)^{0.867}$
20–406	24	200–1500	0.07–1.25	$Nu_b = 0.0061 Re_b^{0.904} \overline{Pr}_b^{0.684} \cdot \left(\frac{\rho_w}{\rho_b}\right)^{0.564}$

In Table 6, the index "b" means that the property is calculated at the mean flow temperature, and the index "w" means that the property is calculated at the internal surface flow temperature of the wall.

6. Problems with SCWO and Suggested Solutions in Literature

The raw material, from which the SCWO installations are made includes large quantities of organic matter soluble and insoluble inorganic salts and at high temperatures and high pressures in the presence of large amounts of oxygen; the materials used in the SCWO plant (notably in reactors and heat exchangers) incur chemical and electrochemical corrosion [107], causing salt precipitation problems. While some companies have commercialized SCWR on a large scale, this technology still poses technical challenges affecting the efficiency, reliability and economics of SCWO processes, especially on a large scale.

6.1. Corrosion

In terms of materials, the main types of corrosion in the supercritical medium are general corrosion, inter-granular corrosion, stress corrosion and pitting corrosion [85,107]. It is affected by the dissociation of acids, bases and salts, the solubility of gases, the solubility of corrosive compounds and the stability of the protective layer [108]. The corrosion rate in SCW systems increases especially in the presence of ionic species [83].

The pH value depends on the equilibrium reaction (Equation (37)) of water dissociation:

$$H_2O \leftrightarrow H^+ + OH^- \quad (37)$$

This reaction is endothermic, which is why the balance shifts to the right side, at high temperature. The concentrations of H^+ and OH^- are approximately three orders of magnitude above values in normal water at a pressure of 25 MPa and at high temperatures, reaching a maximum temperature of approximately 300 °C, so that water can be supposed acidic and alkaline [52].

In fact, reactor corrosion is the main reason for delaying the commercialization of the SCWO processes [7]. Several authors have studied different ways of solving the corrosion problem, Hayward et al. [80] has studied the corrosion of a stainless steel circulation reactor for the oxidation of SW; the impact of oxygenation on corrosion was tested using degassed water, hydrogen peroxide and 3% H_2O_2 solution, for the use of degassed water and hydrogen peroxide, no major modification in the degree of corrosion was noticed, but when H_2O_2 was added to the stream, corrosion increased considerably, at temperatures near the critical temperature, and the highest mean corrosion rate was 0.125 mil/year at 375 °C. They also proved that exhibition of the reactor to the open air between experiments was a reinforcing factor to the corrosion phenomenon of the reactor material. On the other hand, B.R. Foy et al. [109] studied the corrosion of the titanium reactor and hydrogen peroxide is the oxidizing agent. The highest corrosion rate observed was 14 mil/year. Wang et al. [110], studied the comparison between the corrosion of 316 L stainless steel and of "Alloy 625", the reaction was tested in an oxidation process with supercritical water to coking wastewaters treatment, they found pitting corrosion on the area of 316 L stainless steel with a corrosion rate of 0.334 mm/a. Although no important corrosion was observed on the surface of alloy 625, its corrosion rate was 0.052 mm/a. According to this study, the corrosion resistance of alloy 625 was much higher than that of stainless steel 316 L under supercritical conditions.

Table 7 and Figure 18 show the corrosion rates for different reactors. It is clear that the nature of the reactor material is not the only factor influencing these rates, but the operating conditions as well as the corrosion agent do also have important effects.

Regarding economic considerations and corrosion resistance, stainless steels and nickel-based alloys have attracted the interest of researchers more than other materials [81]. So far, no alloy has been developed exclusively for use in SCWO. The principle metallic materials commonly used in supercritical fluid systems included mild steels, stainless steels, and nickel-based alloys [111].

Table 7. Corrosion rates for different SCWO reactors.

Process	Operating Conditions	Corrosion Agent	Max Corrosion Rate mm/yr
Oxidative destruction of chlorocarbons by hydrothermal processing at reasonably high concentrations in a corrosion resistant titanium reactor [106]	200–500 °C, 600 bar	Hydrogen Chloride, Oxidant, Salt	<0.038
Stainless steel 316 circulation reactor for the oxidation of SW [85]	375 °C, 380–400 bar	3% H_2O_2 solutions	0.003175
Alloy 625 reactor [111]	330–550 °C, 400 bar	2.3% HCl/H_2SO_4 solutions Salts, oxidant Salts, oxidant	5.08
Hastelloy C276 reactor [111]	330–550 °C, 400 bar	2.3% HCl/H2SO4 solutions Salts, oxidant	5.08

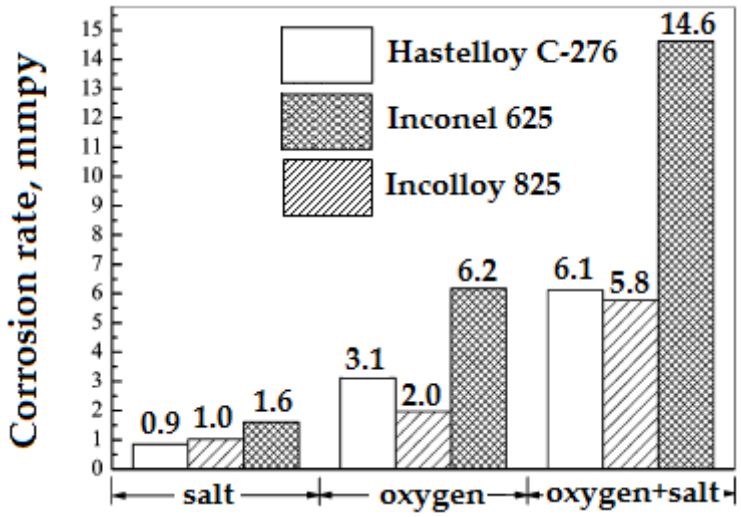

Figure 18. Effects of nickel-based alloys on the corrosion resistance [110].

6.2. Salts Precipitation

As we have already mentioned, due to the unique properties of water under supercritical conditions, organic substances and oxygen have complete solubility, while polar species such as inorganic salts are insoluble and precipitate [18]; this phenomenon is caused by the low dielectric constant of supercritical water and can go as far as shutting off the reactor [54].

Therefore, apart from expensive conventional cleaning methods, special reactor conception and/or practical operational methods are required to find solutions to the problem of salt deposition [112]. Chematur, in its commercial applications, had increased the speed of the fluid to keep the particles in suspension and avoid reactors fouling [113]. Indeed, increasing the operating pressure makes it possible to raise the density of the solution, and subsequently the solubilization of the salts. The problem with this method is that the solubility of the protective oxide layer also increases, which promotes corrosion [52]. P. Kritzer and E. Dinjus [114] stressed that the density of the solution in the reactor must be less than 200 kg/m^3 in order to minimize corrosion and also, they pointed out that the best method to avoid precipitation of salts is to lower the amount of salt present in the feed using separation methods.

Recently, Voisin et al. [115] proposed a new solvent system: hydrothermal molten salt (HyMoS) which can be considered as a very interesting solution to the problem of salt

deposition and corrosion of SCWR. Indeed, this system is able to dissolve a large quantity of inorganic salt in supercritical water and therefore broadens the range of applications for supercritical water.

6.3. Energy Recovery Solution

Since the oxidation reactions in supercritical water are highly exothermic and at the same time require large amounts of energy to reach the high temperature and pressure of the effluents at the input, one of the solutions that could make the process more attractive is the recovery of excess energy from the destruction of waste. Consequently, several authors have emphasized the potential for recovery and integration of the excess energy resulting from the energy of the reaction to the SCWO process, in particular on a large scale, which makes this process more economically profitable.

As we have already mentioned, the energy recovered in the form of heat is used to preheat the supply of reagents and to sustain reaction medium temperatures, which results in system integration. The team of the university of Cádiz, uses an internal resistance system to start the reaction which provides the necessary heat, thereafter, the heat produced by the reaction is used to preheat the supply of liquid and air by using of a heat exchanger consisting of concentric tubes against the current [116]. A simulation was performed to assess the feasibility of energy recovery on an industrial scale of oily waste, in this same process [117]. The results showed that the effluent from the SCWO pilot plant made it possible to produce steam or hot water using the recovered heat from organic waste oxidation. The results were performed for an SCWO industrial installation at 1000 kg/h, with a maximum recovery possibility of 118 kW, or 71% of the energy from wastewater. MD Bermejo et al. [83] realized a study on the production of energy resulting from SCWO of Coal, the effluents leaving the reactor at 650 °C and 30 MPa were expanded in a steam turbine until atmospheric pressure, and the heat removed from the expanded stream is used to preheat partially air and water streams at the inlet. The energy analysis was carried out with two most powerful conventional power plants: pulverized coal power plants and pressurized fluidized bed power plants. The energy yields are 37% in the case of SCWO power station with steam at 650 °C and 30 MPa and 40% with a heating cycle.

Given the design constraints and the actual equipment, it is not technically practicable to filter the vapor under supercritical conditions [24]. Also Florent et al. [24] carried out a simulation with the ProSim Plus software, which made it possible to determine a set of optimal operating conditions to maximize electrical productivity. This maximum efficiency was 1.75% in the case of the biomass SCWO, which is a very low value and not economically rentable [7].

Nawel Outili et al. [117] also carried out a simulation under the SuperPro Designer software, in the case of hydrothermal oxidation in subcritical conditions (WAO) for phenol. They calculated the exact value of the concentration of flow to be treated from which the process becomes autothermal or auto electric. In the WAO process studied, the autothermal point corresponded to 98.78g O_2/L, and the auto electric point corresponded to 118.79 g O_2/L.

Other authors have reported that, apart from organic waste, it is possible to recover the heat given off by the use of secondary alcohols of high calorific value (as auxiliary fuels) used to enhance oxidation reactions and energy efficiency of the SCWO process, and its use for preheating the feed allowing to achieve the energetic auto-sufficient process. For this purpose, Alonso et al. [118] used 2-propanol as fuel for nitrogen-containing compounds, M.D. Bermejo et al. [119] used isopropyl alcohol for ammonia, and Benjumea [7] used ethanol for oil olive mill.

7. Conclusions

The attractive advantages of the supercritical and subcritical properties of water have given rise to new applications. Implementation is no longer limited to the treatment of polluted effluents and is extended to other fields, such as the extraction of compounds of

pharmaceutical, cosmetic and food interest, where the energy recovery of biomass and nanotechnology is concerned.

Oxidation reaction in supercritical water has been used to treat large variations of waste with respect to the environment. Its advantages are the properties acquired by water in the supercritical state acting in its favor as a reaction medium, as well as the excess energy produced by this oxidation which offers the possibility of recovery.

The industrial implementation of this technology has been slowed by the problems of corrosion and precipitation of salts. The operating conditions require high temperature and pressure in SCWO, and the insolubility of salts in supercritical water require the development of construction materials able to resist very aggressive conditions. The reactors developed to take account of these constraints are increasingly complex; the passage through a numerical simulation in order to predict the behavior of a reactor to guide its design is a conceivable and attractive solution.

Kinetic studies of hydrothermal oxidation in supercritical water are limited in number, but further development in this area may lead to the development of models describing a wider range of operating conditions. The results obtained from the use of different hydrodynamic models have shown that CFD is a useful tool for the diagnosis of SCWO reactor mixing problems and for identifying practical measures that could improve reactor performance.

The number and quality of the research in this field, and taking into account the performance of the results in order to solve all the problems that hinder the widespread use of this process on an industrial scale, let us believe that this stage will soon be reached.

Funding: This research received no external funding.

Data Availability Statement: No new data were created.

Conflicts of Interest: The authors declare no conflict of interest.

References

1. Pourmortazavi, S.M.; Saghafi, Z.; Ehsani, A.; Yousefi, M. Application of supercritical fluids in cholesterol extraction from foodstuffs: A review. *J. Food Sci. Technol.* **2018**, *55*, 2813–2823. [CrossRef] [PubMed]
2. Aymonier, C. Traitement Hydrothermal de Déchets Industriels Spéciaux. Données Pour le Dimensionnement D'installations Industrielles et Concepts Innovants de Réacteurs Sonochimique et Électrochimique. Ph.D. Thesis, Université Sciences et Technologies-Bordeaux, Bordeaux France, 2000.
3. Perrut, M. Supercritical fluid applications: Industrial developments and economic issues. *Ind. Eng. Chem. Res.* **2000**, *39*, 4531–4535. [CrossRef]
4. Tarczykowska, A. Green solvents. *J. Educ. Health Sport* **2017**, *7*, 224–232.
5. Hrncic, M.K.; Cor, D.; Verboten, M.T.; Knez, Z. Application of supercritical and subcritical fluids in food processing. *Food Qual. Saf.* **2018**, *2*, 59–67. [CrossRef]
6. Chen, F.; Chen, J.H.; Wu, S.; Rong, S. Cod Removal Efficiency of Aromatic Compounds in Supercritical Water. In Proceedings of the China-Japan International Academic Symposium, Sendai, Japan, 6 March 2000; pp. 115–122.
7. Benjumea, T.J.M. Diseño y Optimización de Plantas de Oxidación en Agua Supercrítica: Aplicación a Residuos Agroalimentarios. Ph.D. Thesis, University of Cádiz, Cádiz, Spain, 2017.
8. Sengers, J.M.H.L.; Erdogan, K. (Eds.) *Supercritical Fluids: Fundamentals for Application*; Kluwer Academic Publishers: New York, NY, USA, 1994.
9. Benmakhlouf, N.; Outili, N.; Meniai, A.-H. Modeling of hydrothermal oxidation in supercritical water oxidation with energy recovery. In Proceedings of the 2016 7th International Renewable Energy Congress (IREC), Hammamet, Tunisia, 22–24 March 2016.
10. Outili, N.; Benmakhlouf, N. An energy recovery study of acetic acid wet air oxidation process. In Proceedings of the 2015 3rd International Renewable and Sustainable Energy Conference (IRSEC), Marrakech, Morocco, 10–13 December 2015.
11. Lachos-Perez, D.; Brown, A.B.; Mudhoo, A.; Martinez, J.; Timko, M.T.; Rostagno, M.A.; Forster-Carneiro, T. Applications of subcritical and supercritical water conditions for extraction, hydrolysis, gasification, and carbonization of biomass: A critical review. *Biofuels* **2017**, *14*, 611–626. [CrossRef]
12. Available online: http://www.portail-fluides-supercritiques.com/fileadmin/userupload/Flash_Infos/IFS_Lettre_info_N$^\circ$8 (accessed on 1 December 2011).
13. Gandhi, K.; Sumit, A.; Kumar, A. Industrial applications of supercritical fluid extraction: A review. *Int. J. Chem. Stud.* **2017**, *5*, 336–340.
14. Oh, C.H. *Hazardous and Radioactive Waste Treatment Technologies Handbook*, 1st ed.; CRC Press: Boca Raton, FL, USA, 2001.

15. Uematsu, M.; Frank, E.U. Static Dielectric Constant of Water and Steam. *Phys. Chem. Ref. Data* **1980**, *9*, 1291–1306. [CrossRef]
16. Loppinet-Serani, A.; Cansell, F.; Frédéric, M.; Mercadier, J. Hydrothermal oxidation of industrial wastewater: An environmental friendly process. In *Récents Progrès en Génie des Procédés*; Société Française du Génie des Procédés (SFGP): St Etienne, France, 2007.
17. Swallow, K.C.; Killilea, W.R.; Malinowski, K.C.; Staszak, C.N. The modar process for the destruction of hazardous organic wastes—Field test of a pilot-scale unit. *J. Waste Manag.* **1989**, *9*, 19–26. [CrossRef]
18. Thomason, T.B.; Hong, G.T.; Swallow, K.C.; Killilea, W.R. The Modar supercritical water oxidation process. *Innov. Waste Treat. Technol. Ser.* **1990**, *I*, 31–42.
19. Bermejo, M.D.; Rincon, D.; Vazquez, V.; Cocero, J.M. Supercritical water oxidation fundamentals and reactor modeling. *Chem. Ind. Chem. Eng. Q.* **2007**, *13*, 79–87. [CrossRef]
20. Marrone, P.A. Supercritical water oxidation-current status of full-scale commercial activity for waste destruction. *J. Supercrit Fluids* **2013**, *79*, 283–288. [CrossRef]
21. Marrone, P.A.; Lachance, R.P.; DiNaro, J.L.; Phenix, B.Q.; Meyer, J.C.; Tester, J.; Peters, W.; Swallow, K.C. Methylene chloride oxidation and hydrolysis in supercritical water as a means of remediation. *ACS Symp. Ser.* **1995**, *608*, 197–216.
22. Moussiere, S. Etude par Simulation Numérique des Ecoulements Turbulents Réactifs dans les Réacteurs d'Oxydation Hydrothermale: Application à un Réacteur Agité Double Enveloppe. PhD Thesis, Université Aix-Marseille-3 Paul Cézanne, Aix-en-Provence, France, 2006.
23. Savage, P.E.; Gopalan, S.; Mizan, T.I.; Martino, C.J.; Brock, E.E. Reactions at Supercritical Conditions: Applications and Fundamentals. *AIChE J.* **1995**, *41*, 1723–1778. [CrossRef]
24. Mancini, F.; Cansell, F.; Marias, F.; Mercadier, J. Hydrothermal oxidation of waste from biomass to generate energy. In Proceedings of the Oral Communication in WasteEng, Albi, France, 17–19 May 2005.
25. Joussot-Dubien, M.C. Etude de L'oxydation Hydrothermal de Déchets Organiques, Cas de Deux Molécules Modèles: Le Dodécane et le Méthanol. Ph.D. Thesis, Université de Bordeaux 1, Bordeaux, France, 1996.
26. Moussiere, S.; Joussot-Dubien, C.; Guichardon, P.; Boutin, O.; Turc, H.-A.; Roubaud, A.; Fournel, B. Modeling of heat transfer and hydrodynamic with two kinetics approaches during supercritical water oxidation process. *J. Supercrit. Fluids* **2007**, *43*, 324–332. [CrossRef]
27. Giulia, G.; Ding Pan, D. A closer look at supercritical water. *Proc. Natl. Acad. Sci. USA* **2013**, *110*, 6250–6251.
28. Marulanda, V. Reacting flow simulations of supercritical water oxidation of BCB-contaminated transformer oil in a pilot plant reactor. *J. Chem. Eng.* **2011**, *28*, 285–294.
29. Loppinet-Serani, A.; Aymonier, C.; Cansell, F. Supercritical water for environmental technologies. *J. Chem. Technol. Biotechnol.* **2010**, *85*, 583–589. [CrossRef]
30. Japas, M.L.; Franck, E.U. High Pressure Phase Equilibria and P VT-Data of the Water-Oxygen System Including Water-Air to 673 K and 250 MPa. *Ber. Bunsenges. Phys. Chem.* **1985**, *89*, 1268–1275. [CrossRef]
31. Fernandez-Prini, R. *High-Temperature Aqueous Solutions: Thermodynamic Properties*, 1st ed.; CRC Press: Boca Raton, FL, USA, 1991.
32. Cocero, M.J. Supercritical Water Oxidation (SCWO). Application to industrial wastewater treatment. High Pressure in Chemical Engineering. *Fundam. Appl.* **2001**, *9*, 509–526.
33. Fourcault, A.; García-Jarana, B.; Sánchez-Oneto, J.; Marias, F.; Portela, J.R. Supercritical water oxidation of phenol with air. Experimental results and modeling. *Chem. Eng. J.* **2009**, *152*, 227–233. [CrossRef]
34. Mercadier, J.; Marias, F.; Vielcazals, S.; Mancini, F.; Bottreau, M.; Cansell, F. Supercritical Water Oxidation of Organic Compounds: Experimental and Numerical Results. *Environ. Eng. Sci.* **2007**, *24*, 1379–1388. [CrossRef]
35. Vielcazals, S.; Mercadier, J.; Marias, F.; Matéos, D.; Bottreau, M.; Cansell, F.; Marraud, C. Modeling and simulation of hydrothermal oxidation of organic compounds. *AIChE J.* **2006**, *52*, 818–825. [CrossRef]
36. Bermejo, M.D.; Fdez-Polanco, F.; Cocero, M.J. Transpiring Wall Reactor for the Supercritical Water Oxidation Process: Operational Results, Modeling and Scaling. In Proceedings of the 10th European Meeting on Supercritical Fluids, Reactions, Materials and Natural Products Processing, Colmar, France, 12 December 2005.
37. Sengers, J.V.; Watson, J.T.R. Improved international formulations for the viscosity and thermal conductivity of water substance. *J. Phys. Chem. Ref. Data* **1986**, *15*, 1291–1312. [CrossRef]
38. Chung, T.H.; Ajlan, M.; Lee, L.L.; Starling, K.E. Generalized Multiparameter Correlation for Nonpolar and Polar Fluid Transport Properties. *Ind. Eng. Chem. Res.* **1988**, *27*, 671–679. [CrossRef]
39. Wagner, W.; Kretzschmar, H.-J. *International Steam Tables, Properties of Water and Steam Based on the Industrial Formulation IAPWS*; Springer: Berlin/Heidelberg, Germany, 1998.
40. Benmakhlouf, N.; Outili, N.; Meniai, A.-H. Modeling and optimization of phenol hydrothermal oxidation in supercritical water. *Int. J. Hydrog. Energy* **2016**, *42*, 12926–129328.
41. Withag, J.A.M.; Sallevelt, J.L.H.P.; Brilman, D.W.F.; Bramer, E.A.; Brem, G. Heat transfer characteristics of supercritical water in a tube: Application for 2D and an experimental validation. *J. Supercrit. Fluids* **2012**, *70*, 156–170. [CrossRef]
42. Serin, J.P.; Mercadier, J.; Marias, F.; Cezac, P.; Cansell, F. Use of CFD for the Design of Injectors for Supercritical Water Oxidation. 2014. Available online: https://www.isasf.net/fileadmin/files/Docs/Colmar/Paper/Rw9.pdf (accessed on 1 December 2022).
43. Miguel, H.; Cifuentes, A.; Ibañez, E. Sub-and supercritical fluid extraction of functional ingredients from different natural sources: Plants, food-by-products, algae and microalgae: A review. *Food Chem.* **2006**, *98*, 136–148.

44. Hanna, P.; Wolak, P.; Złocińska, A. Hydrothermal decomposition of xylan as a model substance for plant biomass waste–hydrothermolysis in subcritical water. *Biomass Bioenergy* **2011**, *35*, 3902–3912.
45. Marta, S.; Fuertes, A.B. Chemical and structural properties of carbonaceous products obtained by hydrothermal carbonization of saccharides. *Chem. Eur. J.* **2009**, *15*, 4195–4203.
46. Marta, S.; Fuertes, A.B.; Mokaya, R. High density hydrogen storage in superactivated carbons from hydrothermally carbonized renewable organic materials. *Energy Environ. Sci.* **2011**, *4*, 1400–1410.
47. Houcinat, I.; Outili, N.; Meniai, A.-H. Parametric study via full factorial design for glycerol supercritical gasification. *Biofuels* **2019**, *13*, 265–278.
48. Istok, G.N.; Zasetsky, A.Y.; Svishchev, I.M. Nucleation of NaCl nanoparticles in supercritical water: Molecular dynamics simulations. *J. Phys. Chem.* **2008**, *112*, 7537–7543.
49. Bagheri, H.; Soltani, R.; Shahmirzaei, M.; Yahyanejad, M.; Fijani, F.; Hashemipour, H. Nanotechnology and supercritical fluids. *J. Fund. Appl. Sci.* **2016**, *8*, 839–859.
50. Benjamin, K.E.; Savage, P.E. Supercritical Water Oxidation of Methylamine. *Ind. Eng. Chem. Res* **2005**, *44*, 5318–5324. [CrossRef]
51. Hatakeda, K.; Ikushima, Y.; Sato, O.; Aizawa, T.; Saito, N. Supercritical water oxidation of polychlorinated biphenyls using hydrogen peroxide. *Chem. Eng. Sci.* **1999**, *54*, 3079–3084. [CrossRef]
52. Bermejo, M.D.; Cocero, M.J. Supercritical Water Oxidation: A Technical Review. *AIChE J.* **2006**, *52*, 3933–3951. [CrossRef]
53. Turbosystems Engineering. *Overview of Supercritical Water Oxidation (SCWO)*; Turbosystems Engineering: San Rafael, CA, USA, 2004.
54. Leybros, A. Etude de la Destruction de Systèmes Polyphasiques en Milieu Eau Supercritique. Ph.D. Thesis, Université de Marseille III, Marseille, France, 2009.
55. Dubois, M.-A.; Dozol, J.; Massiani, C.; Ambrosio, M. Reactivities of polystyrenic polymers with supercritical water under nitrogen or air. Identification and formation of degradation compounds. *Ind. Eng. Chem. Res.* **1996**, *35*, 2743–2747. [CrossRef]
56. Akai, Y.; Yamada, K.; Sako, T. Ion-exchange resin decomposition in supercritical water. *High Press. Res.* **2001**, *20*, 515–524. [CrossRef]
57. Barnes, C.M. *Evaluation of Tubular Reactor Designs for Supercritical Water Oxidation of U.S. Department of Energy Mixed Waste*; Lockheed Idaho Technologies Co.: Idaho Falls, ID, USA, 1994.
58. Gidner, A.; Stenmark, L. *Supercritical Water Oxidation of Sewage Sludge-State of Art*; Chematur Engineering AB: Karlskoga, Sweden, 2000.
59. Lixiong, L.; Chen, P.; Gloyna, E.F. Generalized kinetic model for wet oxidation of organic compounds. *AIChE J.* **1991**, *37*, 1687–1697.
60. Hornton, T.D.; Savage, P.E. Kinetics of phenol oxidation in supercritical water. *AIChE J.* **1992**, *38*, 321–327. [CrossRef]
61. Portela, J.R.; Nebot, E.; Martinez de la Ossa, E. Generalized kinetic models for supercritical water oxidation of cutting oil wastes. *J. Supercrit. Fluids* **2001**, *21*, 135–145. [CrossRef]
62. Zhang, F.; Chen, S.; Xu, C.; Chen, G.; Ma, C. Energy consumption and exergy analyses of a supercritical water oxidation system with a transpiring wall reactor. *Energy Converv. Manag.* **2017**, *145*, 82–92. [CrossRef]
63. Sànchez-Oneto, J.; Portela, J.R.; Nebot, E.; Martinez de la Ossa, E. Hydrothermal oxidation: Application to the treatment of different cutting fluid wastes. *J. Hazard. Mater.* **2007**, *144*, 639–644. [CrossRef] [PubMed]
64. Vadillo, V.; Belin Garcia-Jarana, M.; Sànchez-Oneto, J.; Portela, J.R.; Martinez de la Ossa, E. Simulation of real waste water supercritical water oxidation at high concentration on a pilot plant scale. *Ind. Eng. Chem. Res.* **2011**, *50*, 12512–12520. [CrossRef]
65. Sanchez-Oneto, J.; Mancini, F.; Portela, J.R.; Nebot, E.; Cansell, F.; Martınez de la Ossa, E. Kinetic model for oxygen concentration dependence in the supercritical water oxidation of an industrial wastewate. *Chem. Eng. J.* **2008**, *144*, 361–367. [CrossRef]
66. Benjumea, J.M.; Sanchez-Oneto, J.; Portela, J.R.; Jiménez-Espadafor, F.J.; de la Ossa, E.M. Simulation of supercritical water oxidation reactor in transitory state: Application to time-dependent processes. *J. Supercrit. Fluids* **2016**, *117*, 219–229. [CrossRef]
67. Zhou, L.; Wang, S.; Ma, H.; Gong, Y.; Xu, D. Oxidation of Cu(II) EDTA in supercritical water: Experimental results and modeling. *Chem. Eng. Res. Des.* **2013**, *91*, 286–295. [CrossRef]
68. Portela, J.R.; Nebot, E.; Cansell, F.; de la Ossa, E.M. Kinetic comparison between subcritical and supercritical water oxidation of phenol. *Chem. Eng.* **2001**, *81*, 287–299. [CrossRef]
69. Mateos, D.; Portela, J.R.; Mercadier, J.; Marias, F.; Marrau, C.; François Cansell, F. New approach for kinetic parameters determination for hydrothermal oxidation reaction. *J. Supercrit. Fluids* **2005**, *34*, 63–70. [CrossRef]
70. Tester, J.W.; Webley, P.A.; Holgate, H.R. Revised Global Kinetic Measurements of Methanol Oxidation in Supercritical Water. *Ind. Eng. Chem. Res.* **1993**, *32*, 236–239. [CrossRef]
71. Aymonier, C.; Gratias, A.; Cansell, F. Determination of Hydrothermal Oxidation Reaction Heats by Experimental and Simulation Investigation. *Ind. Eng. Chem. Res.* **2001**, *40*, 114–118.
72. Maharrey, S.P.; Miller, D.R. Quartz Capillary Microreactor for Studies of Oxidation in Supercritical Water. *AIChE J.* **2001**, *47*, 1203–1211. [CrossRef]
73. Koido, K.; Hasegawa, T. Kinetics of ethanol oxidation in high-pressure steam. *J. Therm. Sci. Technol.* **2011**, *6*, 34–42. [CrossRef]
74. Cui, B.; Cui, F.; Jing, G.; Xu, S.; Huo, W.; Liu, S. Oxidation of oily sludge in supercritical water. *J. Hazard. Mater.* **2009**, *165*, 511–517. [CrossRef]

75. Rivas, F.J.; Gimeno, O.; Portela, J.R.; de la Ossa, E.M.; Beltran, F.J. Supercritical Water Oxidation of Olive Oil Mill Wastewaters. *Ind. Eng. Chem. Res.* **2001**, *40*, 3670–3674. [CrossRef]
76. Chkoundali, S.; Sahbi Alaya, S.; Launay, J.C.; Gabsi, S.; Cansell, F. Hydrothermal Oxidation of Olive Oil Mill Wastewater with Multi-Injection of Oxygen: Simulation and Experimental Data. *Environ. Eng. Sci.* **2008**, *25*, 173–179. [CrossRef]
77. Erkonak, H.; Sogut, O.O.; Akgun, M. Treatment of olive mill wastewater by supercritical water oxidation. *J. Supercrit. Fluids* **2008**, *46*, 142–148. [CrossRef]
78. Veriansyah, B.; Jae-Duck Kim, J.D.; Lee, J.C.; Lee, Y.W. OPA oxidation rates in supercritical water. *Hazard. Mater.* **2005**, *B124*, 119–124. [CrossRef]
79. Ploeger, J.M.; Madlinger, D.C.; Tester, J.W. Revised Global Kinetic Measurements of Ammonia Oxidation in Supercritical Water. *Ind. Eng. Chem. Res.* **2006**, *45*, 6842–6845. [CrossRef]
80. Ashraful, A.M.; da Silva, G.A. Detailed chemical kinetic model for the supercritical water oxidation of methylamine: The importance of imine formation. *Int. J. Chem. Kinet.* **2020**, *52*, 701–711. [CrossRef]
81. Tang, X.; Wang, S.; Qian, L.; Ren, M.; Sun, P.; Li, Y.; Yang, J.Q. Corrosion Properties of Candidate Materials in Supercritical Water Oxidation Process. *Adv. Oxid. Technol.* **2016**, *19*, 141–157. [CrossRef]
82. Hayward, T.M.; Svishchev, I.M.; Makhija, R.C. Stainless steel flow reactor for supercritical water oxidation: Corrosion tests. *J. Supercrit. Fluids* **2003**, *27*, 275–283. [CrossRef]
83. Bermejo, M.D.; Cocero, M.J.; Fernández-Polanco, F. A process for generating power from the oxidation of coal in supercritical water. *Fuel* **2004**, *83*, 195–204. [CrossRef]
84. O'Regan, J.; Preston, S.; Dunne, A. Supercritical Water Oxidation of Sewage Sludge-An Update. In Proceedings of the 13th European Biosolids & Organic Resources Conference and Workshop, Manchester, UK, 10–12 November 2008.
85. Mateos, D. Transformation de Matériaux Énergétiques par Oxydation Hydrothermale: Étude Cinétique Globale et Simulation du Procédé en Régime Permanent sur des Composés Modèles. Ph.D. Thesis, Université Sciences et Technologies-Bordeaux I, Bordeaux, France, 2003.
86. Bettinger, J.; Ferland, P.E.; Ferland, E.D. *Demonstration of the Modar Supercritical Water Oxidation Process*; No. CONF-940225-Vol. 2; Arizona University: Tucson, AZ, USA; Coll. of Engineering and Mines, New Mexico State University: University Park, NM, USA; Waste-Management Education and Research Consortium (WERC): Las Cruces, NM, USA; USDOE: Washington, DC, USA, 1994.
87. Bottreau, M.; Momboisse, X.; Bonnaudin, N. The First Plant in France for Industrial Liquid Waste Treatment by Hydrothermal Oxidation Option-H.O.O. 2006. Available online: http://www.isasf.net/fileadmin/files/Docs/Trieste/Papers/Rw07.pdf (accessed on 1 December 2022).
88. Calzavara, Y.; Joussot-Dubien, C.; Turc, H.; Fauvel, E.; Sarrade, S. A new reactor concept for hydrothermal oxidation. *J. Supercrit. Fluids* **2004**, *31*, 195–206. [CrossRef]
89. Xu, D.H.; Wang, S.Z.; Turc, H.; Guo, Y.; Tang, X.Y.; Ma, H.H. A novel concept reactor design for preventing salt deposition in supercritical water. *Chem. Eng. Res. Des.* **2010**, *88*, 1515–1522. [CrossRef]
90. Chen, Z.; Chen, H.; Liu, X.; He, C.; Yue, D.; Xu, Y. An inclined plug-flow reactor design for supercritical water oxidation. *Chem. Eng. J.* **2018**, *343*, 351–361. [CrossRef]
91. Marias, F.; Vielcazals, S.; Cezac, P.; Mercadier, J.; Cansell, F. Theoretical study of the expansion of supercritical water in a capillary device at the output of a hydrothermal oxidation process. *J. Supercrit. Fluids* **2007**, *40*, 208–217. [CrossRef]
92. Malalasekera, W.; Versteeg, H.K. *An Introduction to Computational Fluid Dynamics: The Finite Volume Method*; Pearson: Prentice Hall, NJ, USA, 2007.
93. Roubaud, A.; Moussiere, S.; Fournel, B. 2D and 3D numerical modeling of the reactive turbulent flow in a double shell supercritical water oxidation reactor. *J. Supercrit. Fluids* **2012**, *65*, 25–31.
94. Sierra-Pallaresa, J.; Parra-Santosa, M.T.; García-Sernab, J.; Castroa, F.; Cocero, M.J. Numerical analysis of high-pressure fluid jets: Application to RTD prediction in supercritical reactors. *J. Supercrit. Fluids* **2009**, *49*, 249–255. [CrossRef]
95. Hoffmann, K.A.; Chiang, S.T. *Computational Fluid Dynamics for Engineers*; QA911.H54; Engineering Education System: Austin, TX, USA, 2000.
96. Petrova, R. *Finite Volume Method-Powerful Means of Engineering Design*; InTech: Rijeka, Croatia, 2012.
97. Zhang, Z.Z. Computational Fluid Dynamics Modeling of a Continuous Tubular Hydrothermal Liquefaction Reactor. Master's Thesis, Illinois at Urbana-Champaign, Champaign, IL, USA, 2013.
98. Garcia-Jarana, B.; Sànchez-Oneto, J.; Portela, J.R.; Nebot, E.; de la Ossa, E.M. Simulation of Supercritical Water Oxidation with Air at Pilot Plant Scale. *Int. J. Chem. React.* **2010**, *8*, 1–19. [CrossRef]
99. Akbari, M.; Bazargan, M. A numerical study of supercritical water oxidation of phenol. *J. Iran. Chem. Res.* **2011**, *4*, 187–198.
100. Leybros, A.; Roubaud, A.; Guichardon, P.; Boutin, O. CFD Numerical Modeling of Ion Exchange Resins Supercritical Water Oxidation. *Chem. Eng. Sci.* **2012**, *69*, 70–80. [CrossRef]
101. Zhou, N.; Krishnan, A.; Vogel, F.; Peters, W.A. A computational model for SCW O of organic toxic wastes. *Adv. Environ. Res.* **2000**, *4*, 79–95. [CrossRef]
102. Mokry, S.; Pioro, I.; Farah, A.; King, K.; Gupta, S.; Peiman, W.; Kirillov, P. Development of supercritical water heat-transfer correlation for vertical bare tubes. *Nucl. Eng. Des.* **2011**, *241*, 1126–1136. [CrossRef]
103. Yamagata, K.; Nichikawa, K.; Hasegawa, S.; Fujji, T.; Yochida, S. Forced convective heat transfer to supercritical water flowing in tubes. *Int. J. Heat Mass Trans.* **1975**, *15*, 2575–2593. [CrossRef]

104. Ramasamy, D.; Appusamy, A.; Narayanan, A. Review of the wall temperature prediction capability of available correlations for heat transfer at supercritical conditions of water. *Energy J.* **2013**, *2013*, 159098. [CrossRef]
105. Zoghlami, S. Analyse du Transfert de Chaleur et de la Perte de Pression pour des Ecoulements Supercritiques dans le Réacteur CANDU-SCWR. Ph.D. Thesis, École Polytechnique de Montréal, Montréal, QC, Canada, 2013.
106. Yanga, J.; Wanga, S.; Lia, Y.; Zhangb, Y.; Xua, D. Novel design concept for a commercial-scale plant for supercritical water oxidation of industrial and sewage sludge. *J. Environ. Manag.* **2019**, *233*, 131–140. [CrossRef]
107. Vadillo, V.; Sanchez-Oneto, J.; Portela, J.R.; de la Ossa, E.M. Problems in supercritical water oxidation process and proposed solutions. *Ind. Eng. Chem. Res.* **2013**, *52*, 7617–7629. [CrossRef]
108. Foy, B.R.; Waldthausen, K.; Sedillo, M.A.; Buelow, S.J. Hydrothermal processing of chlorinated hydrocarbons in a titanium reactor. *Environ. Sci. Technol.* **1996**, *30*, 2790–2799. [CrossRef]
109. Wang, Y.; Wang, S.; Guo, Y.; Xu, D.; Gong, Y.; Tang, X.; Ma, H. Corrosion Behavior of 316L Stainless Steel and Alloy 625 in Supercritical Water Oxidation for Coking Wastewater Treatment. *Appl. Mech. Mater.* **2013**, *316–317*, 1037–1040. [CrossRef]
110. Sarrade, S.; Feron, D.; Rouillard, F.; Perrin, S.; Robin, R.; Ruiz, J.-C.; Turc, H.-A. Overview on corrosion in supercritical fluids. *J. Supercrit. Fluids* **2017**, *120*, 335–344. [CrossRef]
111. Faihan Saleh, A. Supercritical Water Oxidation of Nitrogen-Containing Organic Compounds: Process Enhancement Using Isopropyl Alcohol. Ph.D. Thesis, University of Birmingham, Birmingham, UK, 2017.
112. Kulkarni, U.S.; Dixit, S.G. Destruction of Phenol from Wastewater by Oxidation with SO3-2-02. *Ind. Eng. Chem. Res.* **1991**, *30*, 1916–1920. [CrossRef]
113. Kritzer, P.; Dinjus, E. An assessment of supercritical water oxidation (SCWO) Existing problems, possible solutions and new reactor concepts. *Chem. Eng. J.* **2001**, *83*, 207–214. [CrossRef]
114. Voisin, T.; Erriguible, A.; Aymonier, C. A new solvent system: Hydrothermal molten salt. *Sci. Adv.* **2020**, *6*, 1–6. [CrossRef]
115. Vadillo, M.V. Estudio del Proceso de Oxidación en Agua Supercrítica para su Escalamiento Industrial: Implantación de Nuevas Soluciones Tecnológicas, Simulación y Optimización. Ph.D. Thesis, Universidad de Cádiz, Cádiz, Spain, 2012.
116. Jimenez-Espadafor, F.; Portela, J.R.; Vadillo, V.; Sanchez-Oneto, J. Supercritical water oxidation of oily wastes at pilot plant: Simulation for energy recovery. *Ind. Eng. Chem. Res.* **2011**, *50*, 775–784. [CrossRef]
117. Outili, N.; Benmakhlouf, N. Power Recovery Study from Phenol Wet Air Oxidation Process. *Int. J. Elec. Ener.* **2016**, *4*, 24–27. [CrossRef]
118. Alonso, M.J.; Torío, R.E.; Vallelado, D.; Fdz-Polanco, F. Supercritical Water Oxidation in a Pilot Plant of Nitrogenous Compounds: 2-Propanol Mixtures in the Temperature Range 500–750 °C. *Ind. Eng. Chem. Res.* **2000**, *39*, 3707–3716.
119. Bermejo, M.D.; Cantero, F.; Cocero, M.J. Supercritical water oxidation of feeds with high ammonia concentrations Pilot plant experimental results and modeling. *Chem. Eng. J.* **2008**, *137*, 542–549.